Erstgutachterin: PD Dr. Jeanette Lorenz
Zweitgutachter: Prof. Dr. Wolfgang Dünnweber

Search for electroweakinos with the ATLAS detector

Thesis submitted for a doctoral degree in physics
at the faculty of physics of the
Ludwig-Maximilians University
Munich, Germany

Submitted by Eric Schanet, born in Luxembourg
on May 4th, 2021

Supported by the Luxembourg National Research Fund (FNR) (13562317)

Part I

Fundamental concepts

Chapter 1

Theory

The Standard Model of particle physics (SM), introduced in the following section, is a theoretical framework providing a description of nature on the level of elementary particles. Although experimentally well-validated, a number of open questions are left unanswered by the SM. For this reason, the second part of this chapter introduces Supersymmetry, a class of theories that could provide answers to some of these open questions. As searching for Supersymmetry will be the guiding thread throughout this thesis, this chapter will highlight the phenomenological consequences of supersymmetric theories. The mathematical description in the following sections largely follows Refs. [3, 4] for the SM and Refs. [5, 6] for Supersymmetry.

1.1 The Standard Model of particle physics

By the end of the 1920s, quantum mechanics and general relativity had been relatively well established, and the consensus among physicists was that matter is composed of nuclear atoms consisting of electrons and protons. During the 1930s, a multitude of new experimental discoveries and theoretical puzzles excited physicists in, among others, three important directions of research: nuclear physics, cosmic rays and relativistic quantum mechanics [7]. At this time, open questions in these fields included, e.g., the continuous spectrum of the β-decay, the nature of cosmic rays, or the negative energy states in Dirac's relativistic electron theory. As a result of these directions ultimately flowing together, the following decades saw elementary particle physics, emerge as a new field of research.

Since these early times of particle physics, significant progress has been made in describing nature at the subatomic scale. Today, a century later, the resulting theoretical framework, the SM, is the most fundamental, experimentally validated theory of nature known to mankind. It provides an extremely precise description of the interactions of elementary particles, and has been experimentally tested to an unprecedented level of accuracy. Given the remarkable success of the SM, it is not surprising that its history is paved with numerous awards for both experimental and theoretical work. In 1964, the Nobel prize was awarded to Feynman, Schwinger and Tomonoga for their fundamental work on quantum electrodynamics (QED), a quantum field theory allowing the precise calculation of fundamental processes like, e.g., the anomalous magnetic moment of the electron that is known to a relative experimental uncertainty of 2.3×10^{-10} [8]. In 1979, Glashow, Weinberg and Salam were awarded the Nobel prize for their work towards electroweak unification. The most prominent recent progress is undoubtedly the discovery of the Higgs boson, not only resulting in the Nobel prize being

Table 1.1: Names, electric charges (in units of the elementary charge e) and masses (rounded to three significant digits if known to that precision) of all observed fermions in the SM [9]. The symbols used in the following are indicated in parentheses after the particle names.

	generation	particle	electric charge [e]	mass
leptons	1	electron (e)	-1	511 keV
		electron neutrino (ν_e)	0	< 1.1 eV
	2	muon (μ)	-1	106 MeV
		muon neutrino (ν_μ)	0	< 0.19 MeV
	3	tau (τ)	-1	1.78 GeV
		tau neutrino (ν_τ)	0	< 18.2 MeV
quarks	1	up (u)	$\frac{2}{3}$	2.16 MeV
		down (d)	$-\frac{1}{3}$	4.67 MeV
	2	charm (c)	$\frac{2}{3}$	1.27 GeV
		strange (s)	$-\frac{1}{3}$	93 MeV
	3	top (t)	$\frac{2}{3}$	173 GeV
		bottom (b)	$-\frac{1}{3}$	4.18 GeV

awarded to Englert and Higgs, but also completing the SM, roughly 50 years after the existence of the Higgs boson had been postulated.

1.1.1 Particle content of the Standard Model

Apart from the experimentally non-vanishing neutrino masses, the SM successfully describes ordinary matter and their interactions, namely the electromagnetic, weak and strong interactions, leaving gravity as the only fundamental force not described within the SM. The particles in the SM are classified into two main categories, depending on their spin. Particles with half-integer spin follow the Fermi-Dirac statistics and are called *fermions*. As they are subject to the Pauli exclusion principle, they make up ordinary matter. Particles with integer spin are called *bosons*, follow Bose-Einstein statistics and mediate the fundamental interactions.

Fermions are further divided into leptons and quarks, that each come in three generations with increasing masses[†]. Each of the three electrically charged leptons is associated to a corresponding neutral neutrino (more on this association in section 1.1.2). While the SM assumes massless neutrinos, the observation of neutrino oscillations [10] implies the existence of at least two massive neutrinos. By extending the SM to allow non-vanishing neutrino masses, neutrino oscillations can be introduced through lepton generation mixing, described by the Pontecorvo–Maki–Nakagawa–Sakata (PMNS) matrix [11]. Apart from an electric charge, the six quarks also carry a colour charge, of which three types exist: *red*, *green* and *blue*, as well as their respective anti-colours. The mixing in the quark sector through the weak interaction can be described by the Cabibbo–Kobayashi–Maskawa (CKM) matrix [12, 13]. Finally, each fermion comes with its own anti-particle with same mass and spin, but inverted charge-like quantum numbers[§]. All fermions in the SM are listed in table 1.1.

[†] Neutrinos might not exist in a normal mass hierarchy but could also have an inverted mass hierarchy.

[§] The exact nature of anti-neutrinos is still an open question and ties into whether or not the neutrino mass matrix contains non-vanishing Majorana mass terms.

Table 1.2: Names, electric charges (in units of the elementary charge e) and masses (rounded to three significant digits if known to that precision) of all observed bosons in the SM [9]. The symbols used in the following are indicated in parentheses after the particle names.

particle	spin	electric charge [e]	mass
photon (γ)	1	0	0
gluon (g)	1	0	0
$W^{\pm}$	1	± 1	80.4 GeV
Z^0	1	0	91.2 GeV
Higgs boson (h)	0	0	125 GeV

The fundamental forces described by the SM are propagated by bosons with spin-1. The photon γ couples to electrically charged particles and mediates the electromagnetic interaction. As the photon is massless, the electromagnetic force has infinite range. The strong force is mediated by gluons carrying one unit of colour and one unit of anti-colour. Due to colour-confinement, colour charged particles like quarks and gluons cannot exist as free particles and, instead, will form colour-neutral bound states. Although nine gluon states would theoretically be possible, only eight of them are realised in nature—the colour-singlet state $\frac{1}{\sqrt{3}}(|r\bar{r}\rangle + |g\bar{g}\rangle + |b\bar{b}\rangle)$ would result in long-range strong interactions, which have not been observed. Finally, the weak force is mediated by a total of three bosons, two charged $W^{\pm}$ bosons and a neutral Z boson[†]. The mediators of the weak force are massive, resulting in a finitely ranged interaction. They gain their masses through the Higgs mechanism, discussed in chapter section 1.1.2. All bosons known to the SM are listed in table 1.2.

1.1.2 The Standard Model as a gauge theory

Formally, the SM is a collection of a special type of quantum field theories (QFTs), called gauge theories. In the same way that quantum mechanics is the quantisation of dynamical systems of particles, QFT is the application of quantum mechanics to dynamical systems of fields, providing a uniform description of quantum mechanical particles and classical fields, while including special relativity.

In classical mechanics, the fundamental quantity is the action S, which is the time integral of the Lagrangian L, a functional characterising the state of a system of particles in terms of generalised coordinates $q_1, \ldots, q_n$. In field theory, the Lagrangian can be written as spatial integral of a Lagrangian density $\mathcal{L}(\phi_i, \partial_\mu \phi_i)$, which is a function of fields ϕ_i and their spacetime derivatives $\partial_\mu \phi_i$. In the following, the Lagrangian density $\mathcal{L}$ will simply be referred to as the *Lagrangian*. The action can then be written as

$$S = \int L \, \mathrm{d}t = \int \mathcal{L}\left(\phi_i, \partial_\mu \phi_i\right) \mathrm{d}^4 x. \tag{1.1}$$

Using the principle of least action $\delta S = 0$, the equation of motions for each field are given by the Euler-Lagrange-equation,

$$\partial_\mu \left(\frac{\partial \mathcal{L}}{\partial \left(\partial_\mu \phi_i\right)} \right) - \frac{\partial \mathcal{L}}{\partial \phi_i} = 0. \tag{1.2}$$

[†] Due to the electroweak unification, offering a unified description of the electromagnetic and weak interactions in the SM, the Z boson technically has an electromagnetic component and thus is not a *pure* mediator of the weak interaction. Electroweak unification will be discussed in section 1.1.2.

As opposed to the Hamiltonian formalism, the Lagrange formulation of field theory is especially well suited for the relativistic dynamics in particle physics, as it exhibits explicit Lorentz-invariance [4]. This is a direct consequence of the principle of least action, since Lorentz-transformed extrema in the action will still be extrema for Lorentz-invariant Lagrangians.

Symmetries are of central importance in the SM. As Emmy Noether has famously shown in 1918 for classical mechanics, every continuous symmetry of the action has a corresponding conservation law [14]. In the context of classical field theory, each generator of a continuous internal or spacetime symmetry transformation leads to a conserved current, and thus to a conserved charge. In QFTs, quantum versions of Noether's theorem, called Ward–Takahashi identities [15, 16] for Abelian theories and Slavnov–Taylor identities [17–19] for non-Abelian theories relate the conservation of quantum currents and charge-like quantum numbers to continuous symmetries of the Lagrangian.

From a theoretical point of view, the SM is a collection of three gauge theories based on the symmetry group

$$SU(3)_C \otimes SU(2)_\mathrm{L} \otimes U(1)_Y,$$

where $U(n)$ ($SU(n)$) describes (special) unitary groups, i.e. the Lie groups of $n \times n$ unitary matrices (with determinant 1, if special). $SU(3)_C$ generates quantum chromodynamics (QCD), describing the interaction of particles with colour charge C through exchange of gluons, and $SU(2)_\mathrm{L} \otimes U(1)_Y$ generates the electroweak interaction. Here, the subscript 'Y' represents the weak hypercharge, while the subscript 'L' indicates that $SU(2)_\mathrm{L}$ only couples to left-handed particles (right-handed antiparticles).

Feynman diagrams

Transitioning from classical field theory to quantum field theory is typically either done through canonical quantisation or through the usage of the path integral formalism. As only the simplest field theories can be solved analytically, i.e. those containing only free fields and no interactions, perturbation theory is used for calculating scattering cross sections and decay rates for any QFT containing interactions. Any transition matrix can then be written as a series expansion in the coupling constant, with each term represented by Feynman diagrams.

Using appropriate Feynman rules dictating the possible vertices (representing interactions between fields) and propagators (representing the propagation of fields), an infinite number of Feynman diagrams can be written down. All possible combinations of propagators and vertices (i.e. all possible Feynman diagrams) that can be used to connect given incoming and outgoing particles then represent the full perturbation series. Only the lowest order in the series is considered at leading order (LO), the next-lowest at next-to-leading order (NLO), and so on.

Gauge principle

The gauge principle is fundamental to the SM and dictates that the existence of gauge fields is directly related to symmetries under local gauge transformations. QED, being the simplest gauge theory, can be taken to illustrate this important principle. The free Dirac Lagrangian for a single, non-interacting fermion with mass m is given by

$$\mathcal{L}_\mathrm{Dirac} = \bar{\psi}\left(i\gamma^\mu \partial_\mu - m\right)\psi, \tag{1.3}$$

where ψ is a four-component complex spinor field, $\bar{\psi} = \psi^\dagger \gamma^0$, and γ^μ with $\mu = 0, 1, 2, 3$ are the Dirac matrices with the usual anticommutation relations, generating a matrix representation of the Dirac algebra,

$$\{\gamma^\mu, \gamma^\nu\} \equiv \gamma^\mu \gamma^\nu + \gamma^\nu \gamma^\mu = 2\eta^{\mu\nu} \mathbb{1}_4. \tag{1.4}$$

Here, $\eta^{\mu\nu} = \text{diag}(+1, -1, -1, -1)$ is the Minkowski metric. It is worth noting that the free Dirac Lagrangian is invariant under a global $U(1)$ transformation

$$\psi \to \mathrm{e}^{i\theta} \psi, \tag{1.5}$$

where the phase θ is spacetime independent and real-valued. In order to produce the physics of electromagnetism, the free Dirac Lagrangian, has to be invariant under *local* $U(1)$ phase transformations with a spacetime dependent phase $\theta(x)$. This is, however, not the case, as the transformed Lagrangian picks up an additional term from the spacetime derivative of the phase,

$$\mathcal{L}_{\text{Dirac}} \to \mathcal{L}_{\text{Dirac}} - (\partial_\mu \theta(x)) \bar{\psi} \gamma^\mu \psi. \tag{1.6}$$

For the Dirac Lagrangian to become invariant under a local gauge transformation, a new vector field $A_\mu(x)$ has to be introduced and the partial derivative ∂_μ has to be replaced with the covariant derivative D_μ, such that

$$\partial_\mu \to D_\mu \equiv \partial_\mu + ieA_\mu, \tag{1.7}$$

where e can be identified with the elementary charge, representing the coupling of the fermion field to the gauge field A_μ. The prescription of achieving local gauge invariance by replacing ∂_μ with D_μ is called *minimal coupling* and leads to a Lagrangian that is invariant under the transformations

$$\psi \to \mathrm{e}^{i\theta(x)} \psi, \qquad A_\mu \to A_\mu - \frac{1}{e} \partial_\mu \theta(x). \tag{1.8}$$

The modified Lagrangian now includes a term for interactions between the gauge field and the fermion field,

$$\begin{aligned} \mathcal{L} &= \mathcal{L}_{\text{Dirac}} + \mathcal{L}_{\text{int}} \\ &= \bar{\psi} \left(i\gamma^\mu \partial_\mu - m \right) \psi - \left(e\bar{\psi} \gamma^\mu \psi \right) A_\mu, \end{aligned} \tag{1.9}$$

and is indeed invariant under a local phase transformation. Yet, it cannot be complete, as it is still missing a term describing the kinematics of the free gauge field A_μ. For a vector field, the kinetic term is described by the Proca Lagrangian

$$\mathcal{L}_{\text{Proca}} = -\frac{1}{4} F_{\mu\nu} F^{\mu\nu} + \frac{1}{2} m_A^2 A^\nu A_\nu, \tag{1.10}$$

where $F^{\mu\nu} \equiv (\partial^\mu A^\nu - \partial^\nu A^\mu)$ is the field strength tensor that is invariant under the transformation in eq. (1.8). Since $A^\nu A_\nu$ is not invariant under the local transformation of above, the only way to keep the full Lagrangian invariant under a local phase transformation is by requiring $m_A = 0$, i.e. the gauge field A_μ introduced has to be massless, resulting in the Maxwell Lagrangian

$$\mathcal{L}_{\text{Maxwell}} = -\frac{1}{4} F_{\mu\nu} F^{\mu\nu}, \tag{1.11}$$

that ultimately generates the well-known Maxwell equations.

This finally yields the full Lagrangian

$$\begin{aligned}\mathcal{L}_{\text{QED}} &= \mathcal{L}_{\text{Dirac}} + \mathcal{L}_{\text{Maxwell}} + \mathcal{L}_{\text{int}} \\ &= \bar{\psi}\left(i\gamma^\mu\partial_\mu\right)\psi - m\bar{\psi}\psi - \frac{1}{4}F^{\mu\nu}F_{\mu\nu} - \left(e\bar{\psi}\gamma^\mu\psi\right)A_\mu,\end{aligned} \tag{1.12}$$

which can be identified to be the full Lagrangian of QED. The gauge field A_μ introduced is therefore nothing else than the electromagnetic potential with its associated massless particle, the photon. Thus, by applying the gauge principle on the free Dirac Lagrangian, i.e. forcing a global phase invariance to hold locally, a new massless gauge field has to be introduced, including interaction terms with the existing fields in the Lagrangian. In the case of the free Dirac Lagrangian, local gauge invariance produces all of QED.

As Yang and Mills have shown in 1954 [20], requiring a global phase invariance to hold locally is perfectly possible in the case of any continuous symmetry group. Considering a general non-Abelian symmetry group G, represented by a set of $n \times n$ unitary matrices $U(\alpha^1, \ldots, \alpha^N)$, parametrised by N real parameters $\alpha^1, \ldots, \alpha^N$, then a gauge-invariant Lagrangian can be constructed with a similar prescription [3] as previously in the case of $U(1)$.

A total of n fermion fields with mass m are needed, arranged in an n-dimensional multiplet $\Psi = (\psi_1, \ldots, \psi_n)^T$. The free Lagrangian,

$$\mathcal{L}_{\text{free}} = \bar{\Psi}\left(i\gamma^\mu\partial_\mu - m\right)\Psi, \tag{1.13}$$

is invariant under a global phase transformation of the form

$$\Psi(x) \to U(\alpha^1, \ldots, \alpha^N)\Psi(x). \tag{1.14}$$

Each element in the set of transformations U can be written in terms of the group generators T^a as

$$U(\alpha^1, \ldots, \alpha^N) = \mathrm{e}^{i\alpha^a T^a}, \tag{1.15}$$

where the group indices $a = 1, \ldots, N$ are to be summed over. The group generators T^a satisfy the commutation relations

$$[T^a, T^b] = if^{abc}T^c, \tag{1.16}$$

where f^{abc} are the so-called structure constants quantifying the lack of commutativity between the generators. By convention, the basis for the generators T^a is typically chosen such that f^{abc} is completely anti-symmetric [3]. In order to make the Lagrangian invariant under local phase transformations, i.e. under transformations with a set of spacetime-dependent real parameters $\alpha^a(x)$, a vector field $\boldsymbol{W}_\mu$ together with a coupling constant g have to be introduced through the covariant derivative

$$\partial_\mu \to D_\mu = \partial_\mu - ig\boldsymbol{W}_\mu. \tag{1.17}$$

As D_μ acts on the n-dimensional multiplet Ψ, the introduced gauge field $\boldsymbol{W}_\mu$ has to be a $n \times n$ matrix and can thus be expanded in terms of the generators

$$\boldsymbol{W}_\mu(x) = T^a W_\mu^a(x), \tag{1.18}$$

thereby explicitly illustrating, that a total of N gauge fields W_μ^a are introduced through the covariant derivative. Similar to QED above, the covariant derivative also introduces an interaction term of the

form

$$\mathcal{L}_{\text{int}} = g\bar{\Psi}\gamma^{\mu}\boldsymbol{W}_{\mu}\Psi, \tag{1.19}$$

into the Lagrangian in eq. (1.13), coupling the gauge fields W_{μ}^{a} to the fermion multiplet. For infinitesimal $\alpha^{a}(x)$, the gauge fields gauge transform according to

$$W_{\mu}^{a} \rightarrow W_{\mu}^{a} + \frac{1}{g}\partial_{\mu}\alpha^{a} + f^{abc}W_{\mu}^{b}\alpha^{c}, \tag{1.20}$$

where the term with α^{a} looks familiar to the $U(1)$ example and corresponds to the Abelian case, while the term with f^{abc} introduces the non-Abelian structure into the theory [3]. The same non-Abelian structure is again clearly visible when introducing a kinetic term for the gauge fields into the Lagrangian

$$\mathcal{L}_{W} = -\frac{1}{4}F_{\mu\nu}^{a}F^{\mu\nu,a}, \tag{1.21}$$

with the field-strength tensor now $F_{\mu\nu}^{a} = \partial_{\mu}W_{\nu}^{a} - \partial_{\nu}W_{\mu}^{a} + gf^{abc}W_{\mu}^{b}W_{\nu}^{c}$. As was already the case for QED, the above Lagrangian contains Abelian terms quadratic in W, describing the propagation of the free gauge fields. This time, the Lagrangian additionally includes non-Abelian terms cubic and quartic in W, leading to self-interaction of the gauge fields.

Quantum chromodynamics

QCD, the gauge theory describing the strong interaction between quarks and gluons in the SM, is an example for a non-Abelian Yang-Mills theory [20]. QCD is based on the gauge group $SU(3)_{C}$, with the subscript C indicating that the quantum number associated with the symmetry group is the *colour*. Each quark is described by a triplet of fermion fields $q = (q_{r}, q_{g}, q_{b})^{T}$, where the subscripts refer to the three different colours. The symmetry group $SU(3)$ has a total of $n^{2} - 1 = 8$ generators, usually expressed in terms of the Gell-Mann matrices λ^{a} [4]. The covariant derivative introducing the gauge fields G_{μ}^{a} acting on the quark triplets is then

$$D_{\mu} = \partial_{\mu} - ig_{s}\frac{\lambda^{a}}{2}G_{\mu}^{a}, \tag{1.22}$$

with g_{s} the coupling constant of the strong interaction, typically written as $\alpha_{s} = g_{s}^{2}/(4\pi)$ in analogy to the fine-structure constant in QED. Gauge invariance thus introduces a total of $N = 8$ gauge fields that can be identified with the eight gluons, leading to the full Lagrangian of QCD

$$\mathcal{L}_{\text{QCD}} = \sum_{q}\bar{q}(i\gamma^{\mu}D_{\mu} - m_{q})q - \frac{1}{4}G_{\mu\nu}^{a}G^{\mu\nu,a}, \tag{1.23}$$

where $q = u, d, s, c, b, t$ and $G_{\mu\nu}^{a}$ are the gluon field strengths given by

$$G_{\mu\nu}^{a} = \partial_{\mu}G_{\nu}^{a} - \partial_{\nu}G_{\mu}^{a} + g_{s}f^{abc}G_{\mu}^{b}G_{\nu}^{c}. \tag{1.24}$$

As expected from the previous section, $\mathcal{L}_{\text{QCD}}$ contains terms that are cubic and quartic in the gluon fields, resulting in gluon self-interaction in the theory. All possible QCD interaction vertices involving gluons and quarks are shown in fig. 1.1. The gluon self-interaction leads to a number of phenomena unknown to Abelian theories, rendering the kinematics of QCD highly non-trivial.

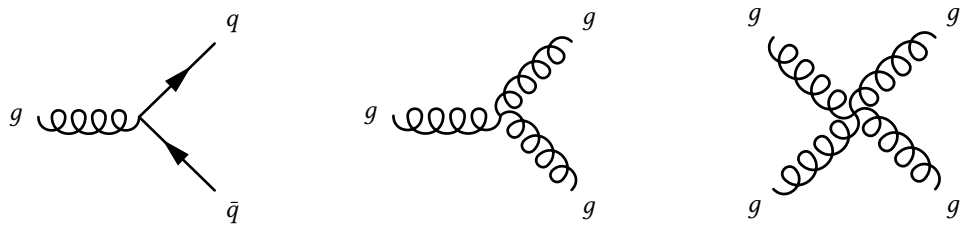

Figure 1.1: Possible vertices in QCD.

In QCD, an effect similar to the electric charge screening in QED happens through quark-antiquark pairs, resulting in a screening of the colour charge. However, the existence of gluon loops in the gluon propagator due to gluon self-interaction creates an opposing *antiscreening* effect of colour charges. At short distances or large momentum scales, colour-charged particles essentially become free particles, a phenomenon called *asymptotic freedom*. In this regime, where α_s is sufficiently small, QCD processes can be calculated using perturbation theory. At large distances or small moment scales, however, α_s becomes large, and gluons interact very strongly with colour-charged particles, meaning that no free gluons or quarks can exist. This phenomenon is called *confinement* and implies that free quarks and gluons will be subject to *hadronisation*, i.e. form colourless bound states by combining with other quarks or gluons (that can be created from the vacuum). In a particle detector, hadronisation manifests itself as collimated showers of particles, called *jets*. At momentum scales where the strong coupling constant α_s becomes large ($\alpha_s \approx \mathcal{O}(1)$), QCD processes can no longer be calculated using perturbation theory and instead lattice QCD [21, 22] is used.

Electroweak interaction

During the 1960s, Glashow, Weinberg and Salam [23–25] developed a unified theory of the electromagnetic and weak interactions, based on the $SU(2)_\mathrm{L} \otimes U(1)_Y$ symmetry group. Known already experimentally from the Wu experiment [26] in 1956, weak interaction violates parity, i.e. the symmetry transformations have to act differently on the left-handed and right-handed fermion fields. The left- and right-handed components of a fermion field can be projected out using

$$\psi_\mathrm{L} = \frac{1-\gamma^5}{2}\psi, \qquad \psi_\mathrm{R} = \frac{1+\gamma^5}{2}\psi, \tag{1.25}$$

with $\gamma^5 = i\gamma^0\gamma^1\gamma^2\gamma^3$. As the weak interaction only acts on left-handed fermions, they can be ordered as $SU(2)$ doublets

$$\begin{pmatrix}\nu_e\\ e\end{pmatrix}_\mathrm{L}, \quad \begin{pmatrix}u\\ d\end{pmatrix}_\mathrm{L}, \qquad \begin{pmatrix}\nu_\mu\\ \mu\end{pmatrix}_\mathrm{L}, \quad \begin{pmatrix}c\\ s\end{pmatrix}_\mathrm{L}, \qquad \begin{pmatrix}\nu_\tau\\ \tau\end{pmatrix}_\mathrm{L}, \quad \begin{pmatrix}t\\ b\end{pmatrix}_\mathrm{L}. \tag{1.26}$$

The quantum number associated with $SU(2)$ symmetry transformations is called weak isospin I with the third component denoted as I_3. Fermion doublets have $I = 1/2$, with the upper component having $I_3 = 1/2$ and the lower component $I_3 = -1/2$. Right-handed fermion fields have $I = 0$, i.e. are singlet states in weak isospin space

$$e_\mathrm{R},\ u_\mathrm{R},\ d_\mathrm{R}, \qquad \mu_\mathrm{R},\ c_\mathrm{R},\ s_\mathrm{R}, \qquad \tau_\mathrm{R},\ t_\mathrm{R},\ b_\mathrm{R}, \tag{1.27}$$

and thus do not couple to the weak interaction. In the electroweak theory, neutrinos are assumed to be strictly massless, therefore no right-handed neutrino singlets exist.

The fermion doublets can be written in a free Lagrangian similar to eqs. (1.3) and (1.13),

$$\mathcal{L} = \bar{\psi}_\mathrm{L} i\gamma^\mu \partial_\mu \psi_\mathrm{L}, \tag{1.28}$$

with one crucial difference—the omission of the fermion masses. As $\bar{\psi}\psi = \bar{\psi}_\mathrm{L}\psi_\mathrm{R} + \bar{\psi}_\mathrm{R}\psi_\mathrm{L}$, mass terms would mix left- and right-handed terms and break gauge invariance. Section 1.1.2 will illustrate how fermion masses will instead be generated in the electroweak theory. For left-handed fermion fields, local $SU(2)_\mathrm{L}$ transformations can be written as

$$\psi_\mathrm{L} \rightarrow \exp\left(i g_2 \alpha^a \frac{\sigma^a}{2}\right) \psi_\mathrm{L}, \tag{1.29}$$

where g_2 is the coupling constant, α^a (with $a = 1, 2, 3$) are real parameters and the Pauli matrices σ^a are the generators of $SU(2)_\mathrm{L}$. By introducing the covariant derivative $D_\mu = \partial_\mu + i g_2 \frac{\sigma^a}{2} W_\mu^a$ and including the usual kinetic term for the gauge fields, the Lagrangian becomes invariant under $\mathrm{SU(2)_L}$ transformations and reads

$$\mathcal{L} = \bar{\psi}_\mathrm{L} i\gamma^\mu D_\mu \psi_\mathrm{L} - \frac{1}{4} W^a_{\mu\nu} W^{\mu\nu,a}, \tag{1.30}$$

with the gauge field strength tensors $W^a_{\mu\nu} = \partial_\mu W^a_\nu - \partial_\nu W^a_\mu + g_2 \epsilon^{abc} W^b_\mu W^c_\nu$, where ϵ^{abc} are the structure constants. As previously in the case of QCD, the non-Abelian structure of the symmetry group causes self-interactions of the gauge fields.

In order to include electromagnetic interactions, the weak isospin group is extended with the $U(1)_Y$ group, corresponding to the multiplication of a phase factor $e^{i\alpha \frac{Y}{2}}$ to each of the preceding doublets and singlets. Here, Y is the weak hypercharge as given by the Gell-Mann–Nishijima relation [27–29],

$$Q = I_3 + \frac{Y}{2}, \tag{1.31}$$

with Q the electric charge. As will be discussed in section 1.1.2, the spontaneous breaking of the $SU(2)_\mathrm{L} \otimes U(1)_Y$ gauge symmetry will recover the electromagnetic gauge group $U(1)_\mathrm{em}$ [4].

By modifying the covariant derivative to include a $U(1)_Y$ gauge field and ensuring that $U(1)_Y$ acts the same on left-handed and right-handed fermions with coupling constant g_1, it can be written as $D_\mu = \partial_\mu + i g_2 \frac{\sigma^a}{2} W^a_\mu + i g_1 \frac{Y}{2} B_\mu$ for left-handed fermions and $D_\mu = \partial_\mu + i g_1 \frac{Y}{2} B_\mu$ for right-handed fermions. The full electroweak Lagrangian then is

$$\begin{aligned} \mathcal{L}_\mathrm{electroweak} = &\sum_j \bar{\psi}^j_\mathrm{L} i\gamma^\mu \left(\partial_\mu - i g_2 \frac{\sigma^a}{2} W^a_\mu + i g_1 \frac{Y}{2} B_\mu\right) \psi^j_\mathrm{L} \\ &+ \sum_j \bar{\psi}^j_\mathrm{R} i\gamma^\mu \left(\partial_\mu + i g_1 \frac{Y}{2} B_\mu\right) \psi^j_\mathrm{R}, \end{aligned} \tag{1.32}$$

where $B_{\mu\nu} = \partial_\mu B_\nu - \partial_\nu B_\mu$, and the two sums run over the left- and right-handed fermions, respectively.

Spontaneous symmetry breaking

In the electroweak theory a total of three vector fields W_μ^a and one vector field B_μ are associated with the gauge groups $SU(2)_\mathrm{L}$ and $U(1)_Y$, respectively. As has been shown explicitly through the example of QED in section 1.1.2, the gauge fields need to be massless for the resulting Lagrangian to be gauge invariant under the respective symmetry group. In addition, the electroweak symmetry group does not allow for fermion masses. Both gauge bosons of the weak interaction and the fermions are, however, manifestly massive, and therefore the electroweak symmetry has to be broken in the SM.

The spontaneous symmetry breaking of the $SU(2)_\mathrm{L} \otimes U(1)_Y$ gauge group is achieved through the Brout–Englert–Higgs mechanism [30–32]. In the SM, an isospin doublet of complex scalar fields, called Higgs doublet, is introduced

$$\Phi(x) = \begin{pmatrix} \phi^+(x) \\ \phi^0(x) \end{pmatrix}. \tag{1.33}$$

The Higgs doublet has hypercharge $Y = 1$, and thus, according to the Gell-Mann–Nishijima relation, ϕ^+ has electric charge +1 while ϕ^0 is electrically neutral. With the covariant derivative introduced in section 1.1.2, the Higgs doublet gets corresponding terms in the SM Lagrangian,

$$\mathcal{L}_h = (D_\mu \Phi)^\dagger (D^\mu \Phi) - V(\Phi), \tag{1.34}$$

where $V(\Phi)$ is a gauge invariant potential of the form

$$V(\Phi) = -\mu^2 \Phi^\dagger \Phi + \frac{\lambda}{4} (\Phi^\dagger \Phi)^2. \tag{1.35}$$

For positive and real parameters μ^2 and λ, this potential has the form of a *Mexican hat* and an infinite number of minima for field configurations with $\Phi^\dagger \Phi = 2\mu^2/\lambda$. In the vacuum, i.e. in the ground state of the theory with minimal potential energy of the field, one of these minima is chosen such that the Higgs receives a vacuum expectation value (VEV),

$$\langle \Phi \rangle = \frac{1}{\sqrt{2}} \begin{pmatrix} 0 \\ v \end{pmatrix} \qquad \text{with} \quad v = \frac{2\mu}{\sqrt{\lambda}} \approx 246\,\mathrm{GeV}. \tag{1.36}$$

Equation (1.36) is neither invariant under a $SU(2)_\mathrm{L}$ transformation of the form $U = \exp(i\alpha^a \frac{\sigma^a}{2})$, nor under a $U(1)_Y$ phase factor of the form $\exp(i\alpha \frac{Y}{2})$. Thus, the Lagrangian has a symmetry that the vacuum state does not share, thereby spontaneously breaking the $SU(2)_\mathrm{L} \otimes U(1)_Y$ symmetry. As the VEV of ϕ^+ vanishes and ϕ^0 is invariant under $U(1)_\mathrm{em}$, the $SU(2)_\mathrm{L} \otimes U(1)_Y$ symmetry group is broken down to $U(1)_\mathrm{em}$ [3].

The Higgs doublet can be expressed as excitations around the ground state

$$\Phi(x) = \frac{1}{\sqrt{2}} \begin{pmatrix} \phi_1(x) + i\phi_2(x) \\ v + h(x) + i\chi(x) \end{pmatrix}, \tag{1.37}$$

where h, χ, ϕ_1 and ϕ_2 are real-valued scalar fields with vanishing VEVs. Inserting eq. (1.37) back into the potential $V(\Phi)$ in eq. (1.35) yields

$$V = \mu^2 h^2 + \frac{\mu^2}{v} h(h^2 + \chi^2 + \phi_1^2 + \phi_2^2) + \frac{\mu^2}{4v^2} (h^2 + \chi^2 + \phi_1^2 + \phi_2^2)^2, \tag{1.38}$$

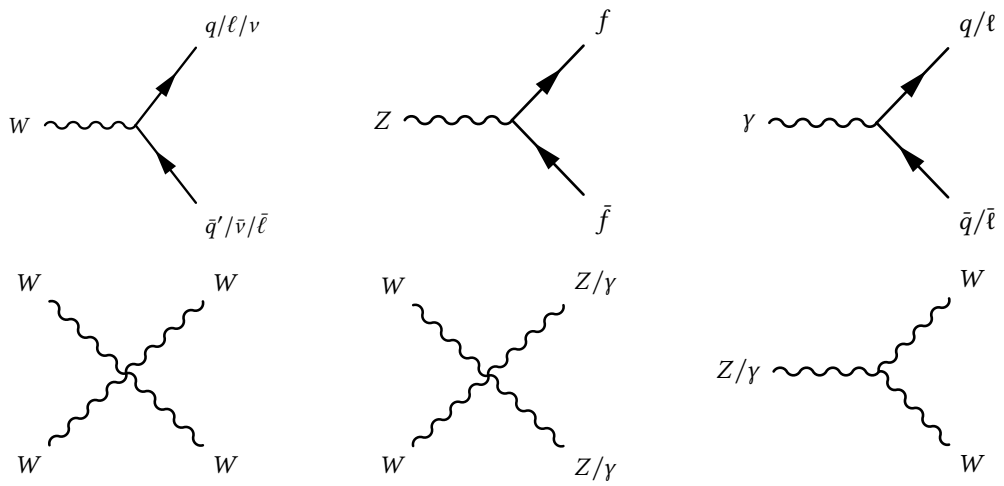

Figure 1.2: Possible vertices in the electroweak interaction.

where only h gets a mass term, thus corresponding to an electrically neutral scalar particle with mass $m_h = \sqrt{2}\mu$. The other scalar fields remain massless, which is in accordance with the Nambu-Goldstone theorem [33, 34], stating that every spontaneously broken continuous symmetry generates a massless Goldstone boson. These bosons are unphysical and can be gauged away through a $SU(2)_\mathrm{L}$ transformation, such that the expansion around the vacuum from eq. (1.37), involves only the physical scalar h in the so-called *unitary gauge* [3].

Inserting eq. (1.37) and the potential V from eq. (1.38) back into the Lagrangian $\mathcal{L}_h$ in eq. (1.34) leads to mass terms for the gauge fields through their couplings to the h field. The *physical* fields corresponding to the physically observable $W^\pm$, Z and γ bosons in the electroweak theory are then given by the linear combinations

$$\begin{aligned} W_\mu^\pm &= \frac{1}{\sqrt{2}}(W_\mu^1 \mp iW_\mu^2) && \text{with} \quad m_W = \frac{g_2}{2}v, \\ Z_\mu &= \cos\theta_W W_\mu^3 - \sin\theta_W B_\mu && \text{with} \quad m_Z = \frac{1}{2}\sqrt{g_1^2 + g_2^2}v, \\ A_\mu &= \sin\theta_W W_\mu^3 + \cos\theta_W B_\mu && \text{with} \quad m_A = 0, \end{aligned}$$

where θ_W is the weak mixing angle. It is related to the masses of the W and Z bosons and the electroweak coupling constants by

$$\cos\theta_W = \frac{g_2}{\sqrt{g_1^2 + g_2^2}} = \frac{m_W}{m_Z}. \tag{1.39}$$

In the SM the $W^\pm$ and Z bosons hence acquire masses through spontaneous breaking of the electroweak gauge symmetry $SU(2)_\mathrm{L} \otimes U(1)_Y$ through the Higgs mechanism. The massless photon field A_μ associated with the electromagnetic $U(1)_\mathrm{em}$ gauge symmetry is automatically recovered. All possible vertices between fermions and the physical gauge bosons described by the electroweak theory are shown in fig. 1.2.

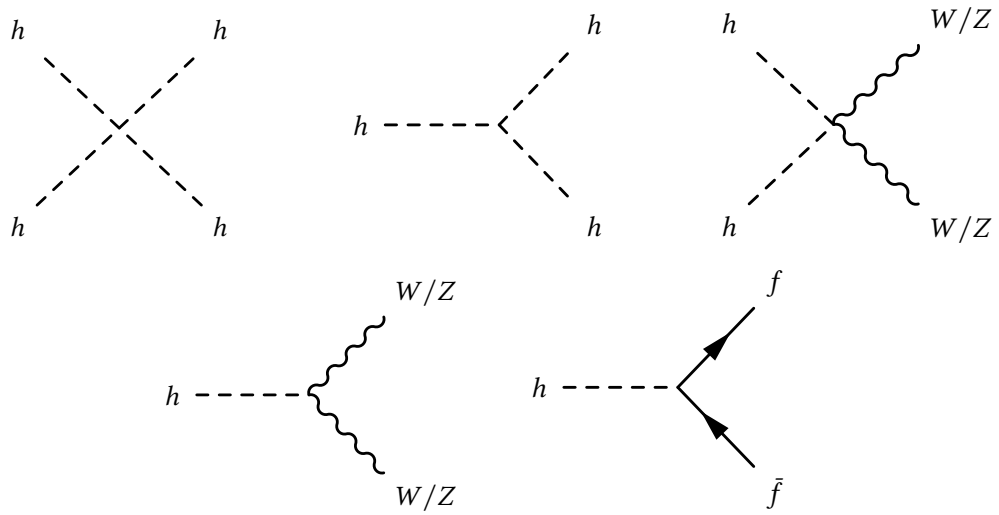

Figure 1.3: Possible vertices involving the Higgs boson.

Furthermore, the masses of fermion fields are related to gauge-invariant Yukawa interactions with the Higgs field. For one fermion generation, the respective Yukawa terms in the Lagrangian are

$$\mathcal{L}_{\text{Yukawa,gen}} = -\lambda_\ell \bar{L}_\text{L} \Phi \ell_\text{R} - \lambda_d \bar{Q}_\text{L} \Phi d_\text{R} - \lambda_u \bar{Q}_\text{L} \Phi^\dagger u_\text{R} + \text{h.c.}, \tag{1.40}$$

where λ_f with $f = \ell, d, u$ are the dimensionless Yukawa couplings and $L_\text{L} = (\nu_\text{L}, \ell_\text{L})^T$ and $Q_\text{L} = (u_\text{L}, d_\text{L})^T$ are the left-handed lepton and quark doublets, respectively. The non-vanishing VEV of the Higgs field then gives rise to fermion mass terms of the form

$$m_f = \lambda_f \frac{v}{\sqrt{2}}, \tag{1.41}$$

yielding fermion couplings to the Higgs field proportional to the fermion masses m_f. All SM interaction vertices involving the Higgs boson are shown in fig. 1.3.

When introducing all three fermion generations, additional Yukawa terms mixing fermions of different generations appear in the Lagrangian [3]. The terms involving quark fields can be parametrised using the CKM matrix V_CKM [12, 13], quantifying the transition probability between quark generations. Since no right-handed neutrinos exist in the SM, no generation mixing in the lepton sector occurs and hence no neutrino mass terms are allowed in the SM. Neutrino oscillations have, however, been observed experimentally, thus at least two massive neutrino generations need to exist. Their mixing can be described[†] with the PMNS matrix [11], allowing neutrinos to acquire mass e.g. through the see-saw mechanism [35].

1.1.3 Renormalisation and divergencies

At lowest order in the perturbative expansion, the momenta of the internal lines in the Feynman diagrams are fixed by the external particles. For higher orders where the diagrams involve loops, the momenta of the internal lines need to be integrated over as they are not fixed by energy-momentum

[†] Technically, this is already an extension of the SM.

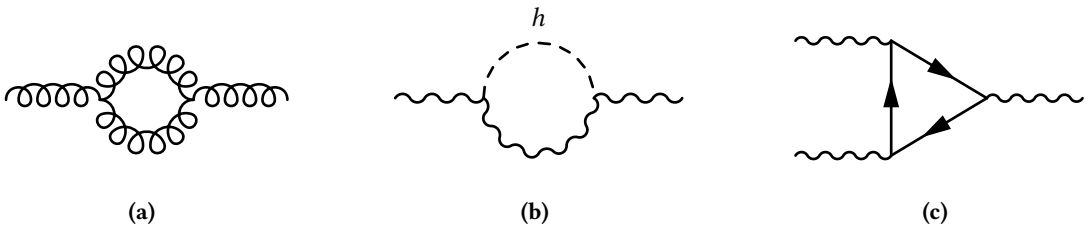

Figure 1.4: Examples of loop corrections to (a) the gluon propagator, (b) the W or Z propagator and (c) the cubic gauge boson vertex.

conservation. Some examples of loop corrections to propagators and vertices are shown in fig. 1.4. As each vertex in the Feynman diagrams is associated with a coupling constant that is usually much smaller than 1 (apart from the non-perturbative regime of QCD), higher orders in the perturbative expansion contribute less and less to the total amplitude of the full expansion.

The momentum integrals in loop corrections, however, lead to *ultraviolet divergencies* for large momenta. In order to eliminate the divergencies, the integrals have to be *regularised*, e.g. by applying a cut-off scale Λ, or calculating the integrals in a number $D = 4 - \epsilon$ of dimensions where they converge. The potential divergencies are then absorbed in parameters of the Lagrangian, such as coupling constants and masses, after which the regulator is removed again (e.g. by setting $\epsilon \to 0$) and a *renormalisation* procedure is applied, replacing the bare parameter values with the physical, measured values [3]. Renormalisation effectively absorbs the effects of quantum fluctuations, acting on much smaller scales than the scale of the given problem, into the parameters of the theory. As Veltmann and t'Hooft [36, 17] have shown, all Yang-Mills theories with massive gauge fields are renormalisable, rendering the SM as a whole a renormalisable theory.

1.2 Supersymmetry

Originally developed in the late 1960s and early 1970s as an attempt to combine the Poincaré group with internal symmetries into a single symmetry group [37], Supersymmetry (SUSY) is a class of theories transforming fermionic states into bosonic ones, and vice-versa. Since its theoretical discovery, driven purely by theoretical developments rather than by pressure of existing data [37], Supersymmetry (SUSY) was found to have far-reaching phenomenological consequences that could solve some of the shortcomings of the SM.

This section starts with an overview of the shortcomings of the SM and illustrates how they could be solved by supersymmetric theories. This is followed by an introduction to the mathematical description and phenomenological consequences of SUSY. While the following sections are intended to highlight the most important concepts and relations, a much more complete and detailed introduction to SUSY can be found, e.g., in Refs. [5, 6].

1.2.1 Shortcomings of the Standard Model

Although the SM is a remarkably successful theory that is able to predict and describe the interactions between elementary particles with unprecedented precision, there are still phenomena in nature that cannot be suitable understood within the theoretical framework of the SM.

Those limitations and open questions are the reason for numerous searches looking for new physics beyond the SM, such as the one presented in this thesis. Some of these open questions are described in the following.

Dark Matter

The existence of dark matter (DM), i.e. non-luminous and non-absorbing matter is nowadays well established [9]. Some of the earliest hints for the existence of dark matter (DM) came from the observation that the rotation curves of luminous objects are not consistent with the expected velocities based on the gravitational attraction of the visible objects around them. Zwicky already postulated in 1933 the existence of DM [38] based on rotation curves of galaxies in the Coma cluster. In 1970, Rubin measured rotation curves of spiral galaxies [39], revealing again a significant disagreement with the theoretically expected curves given the visible matter in the galaxies. Based on Newtonian dynamics, the circular velocity of stars outside the bulge of galaxies is expected to fall off with increasing radius as $v(r) \propto 1/\sqrt{r}$ [40]. Rubin's observations, however, revealed that the velocities of stars outside the bulge stay approximately constant, strongly suggesting the existence of a non-luminous (or *dark*) matter halo around the galaxies. Surveys of galaxy clusters and observations of gravitational lensing effects, e.g., in the bullet cluster [41] or the Abell 1689 cluster [42], have since then further consolidated the existence of large accumulations of non-luminous matter in the universe.

The anisotropies in the cosmic microwave background (CMB), studied by the COBE [43, 44], WMAP [45, 46] and Planck missions [47] are well described by the Lambda Cold Dark Matter (ΛCDM) model [48], which includes a density for cold dark matter. Planck's latest results [49] for the cold DM relic density $\Omega_c h^2$ and baryonic density $\Omega_b h^2$ of

$$\begin{aligned} \Omega_c h^2 &= 0.1200 \pm 0.0012, \\ \Omega_b h^2 &= 0.02237 \pm 0.00015, \end{aligned} \tag{1.42}$$

suggest that ordinary baryonic matter only makes up $\sim 4.9\%$ of the universe's matter content, while DM accounts for $\sim 26.1\%$[†].

Candidates for cold DM need to satisfy certain conditions: they have to be stable on cosmological timescales (otherwise they would have decayed by now), they have to couple only very weakly to the electromagnetic interaction (if at all, otherwise they would be *luminous* matter) and they need to have the right relic density. Analyses of structure formations in the Universe have furthermore shown that most DM should have been *cold*, i.e. non-relativistic, at the beginning of galaxy formation [40]. Candidates for DM particles are e.g. sterile neutrinos, axions, primordial black holes, or weakly interacting massive particles (WIMPs).

In the SM, the only DM candidate particle is the neutrino. Given the upper limits on the neutrino masses, an upper bound on their relic density can be computed, revealing that neutrinos are not abundant enough to be a dominant component of DM [40]. Furthermore, due to their low masses, neutrinos would still have been relativistic particles at the beginning of galaxy formation, preventing the *bottom-up*[§] structure formation, favoured by a cold DM dominated universe.

[†] The remaining $\sim 69\%$ are taken up by *dark energy*, the nature of which is still an open question.

[§] The *bottom-up* structure formation begins with small objects that subsequently merge into ever larger structures and corresponds to the structure formation process favoured in a universe dominated by cold DM.

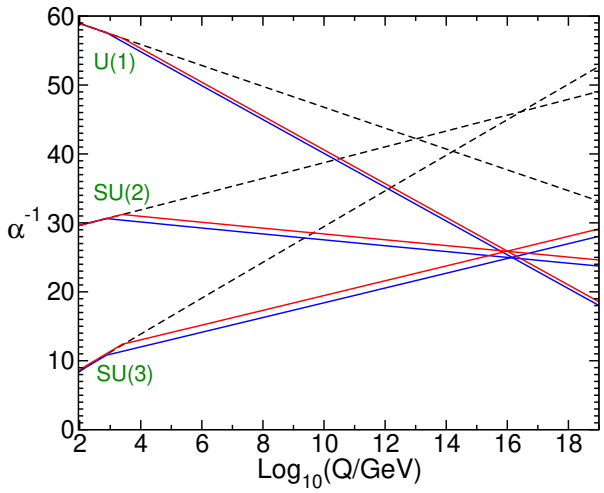

Figure 1.5: Evolution of the inverse coupling constants in the SM (dashed lines) and the MSSM (solid lines) in function of the energy scale Q. Here, the masses of the supersymmetric particles are treated as common threshold and varied between 750 GeV (blue lines) and 2.5 TeV (red lines). Figure taken from Ref. [5].

Many beyond the Standard Model (BSM) theories naturally predict new WIMPs with masses in the GeV to TeV range. In many SUSY models with exact R-parity conservation (a quantity introduced in section 1.2.5), the lightest supersymmetric particle is neutral and stable and could be a good candidate for DM.

Unification of forces

Although the SM provides a good description of nature up to the energy scale probed with today's accelerators, some of its peculiar aspects hint to a more fundamental theory. A prominent example is the question why the electric charges of the electrons and the charges of the quarks in the protons and neutrons in the nuclei exactly cancel, making for electrically neutral atoms [3]. Or in other words: why are the charges of all observed particles simple multiples of the fundamental charge? And why are they quantised in the first place?

An explanation to many of these peculiarities comes naturally when describing the SM as a unified theory with a single non-Abelian gauge group, e.g. $SU(5)$ [50]. The larger symmetry group with a single coupling constant is then thought to be spontaneously broken at very high energy, such that the known SM interactions are recovered at the lower energies probed in today's experiments. In such a grand unified theory (GUT), the particles in the SM are arranged in anomaly-free[†], irreducible representations of the gauge group, thereby, for example, naturally ensuring the fractional charges of quarks [4].

In the SM, the coupling constants run towards each other with increasing energy scale, but never exactly meet. In the Minimal Supersymmetric Standard Model (MSSM), introduced in section 1.2.5, the running couplings meet within their current uncertainties if the supersymmetric particles are at the TeV scale, hinting that a supersymmetric GUT could be a good candidate for describing physics at the unification scale. Figure 1.5 shows that the running coupling constants in the MSSM are modified such that they meet at 10^{16} GeV.

[†] In the sense that loop corrections do not break symmetries the Lagrangian has.

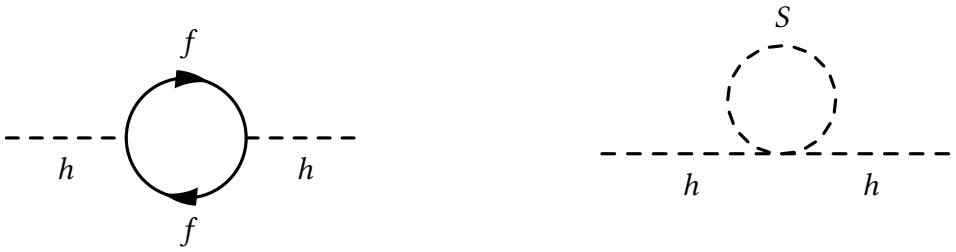

(a) (b)

Figure 1.6: A massive fermion (a) and a hypothetical massive scalar particle (b) coupling to the Higgs boson.

The Hierarchy Problem

As the SM is a renormalisable gauge theory, finite results are obtained for all higher-order loop corrections, making the SM a theory that is, in principle, well-defined up to infinite energies. In renormalisation terms, this means that the cut-off scale Λ is theoretically allowed to go to arbitrarily high values. It is clear though, that the SM cannot be a complete theory of nature and that, at some unknown high-energy scale Λ, *new physics* has to appear. At the very least, a new theoretical framework becomes necessary at the Planck scale $M_P \approx 10^{19}$ GeV [6], where quantum gravitational effects can no longer be ignored.

The mass parameters of fermions and massive vector bosons are protected from large quantum corrections by chiral symmetry and gauge symmetry, respectively [51]. The mass parameter of the scalar Higgs field, on the other hand, receives loop corrections proportional at least to the scale at which new physics sets in. The Yukawa coupling of the Higgs field to a fermion f with mass m_f, depicted in fig. 1.6(a), yields a one-loop correction term to the Higgs square mass [6] given by

$$\Delta m_h^2 = -\frac{\lambda_f^2}{8\pi^2}\Lambda^2 + \dots . \tag{1.43}$$

The Higgs mass thus quadratically diverges with the scale Λ. If the SM is to be valid up to the Planck scale, then $\Lambda = M_P$, and the correction to the Higgs squared mass becomes more than 10^{30} times larger than the expected value in the order of $(10^2\ \text{GeV})^2$ [5]. Similar quantum corrections arise from the Higgs quartic coupling to a heavy scalar boson S with mass m_S, shown in fig. 1.6(b), yielding a one-loop correction [6] given by

$$\Delta m_h^2 = \frac{\lambda_S}{16\pi^2}\Lambda^2 + \dots . \tag{1.44}$$

In order to obtain the experimentally measured value of the Higgs mass, the quantum corrections to the bare Higgs parameter have to be tuned in such a way that they almost cancel, leading to a *fine-tuning* problem that is considered to be unnatural.

Interestingly, the terms quadratically divergent in Λ in eq. (1.43) and eq. (1.44) enter with opposite signs. If, for every fermionic loop, there are two bosonic loops with $\lambda_S = \lambda_f^2$, the quadratically diverging terms neatly cancel. As will be discussed, this is exactly the case in supersymmetric theories. Additional correction terms omitted above are at most logarithmic in Λ, and cancel if the scalar bosons and the fermion have the same masses (this is further discussed in section 1.2.5).

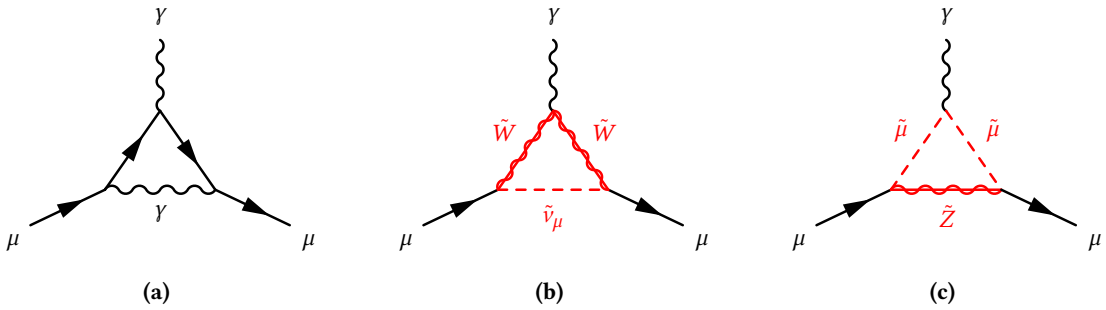

Figure 1.7: Electromagnetic (a) and supersymmetric (b), (c) contributions to a_μ. Supersymmetric particles are drawn in red. Adapted from Ref. [53].

Anomalous magnetic moment of the muon

One of the longest standing disagreements between experiment and theory in the SM is the anomalous magnetic moment of the muon [9]. The magnetic moment of the muon $\vec{\mu}_\mu$ is related to its intrinsic spin $\vec{S}$ through the gyromagnetic ratio g_μ by

$$\vec{\mu}_\mu = g_\mu \frac{q}{2m} \vec{S}. \tag{1.45}$$

For a structureless spin-1/2 particle with mass m and charge $q = \pm e$, the gyromagnetic ratio is $g_\mu = 2$ [52]. Loop corrections coupling the muon spin to virtual fields cause small deviations, parameterised by the anomalous magnetic moment

$$a_\mu = \frac{1}{2}(g_\mu - 2). \tag{1.46}$$

The anomalous magnetic moment can be precisely predicted within the SM and experimentally measured with high accuracy. A comparison between experimental data and theoretical prediction thus directly tests the SM at quantum loop level and may hint to effects from new physics in case of discrepancies [53]. In the SM, the most dominant contribution to a_μ comes from QED corrections involving photon and fermion loops. An exemplary diagram is shown in fig. 1.7(a). Weak contributions involving the heavy $W^\pm$, Z and Higgs particles are suppressed by their masses [54]. Although the contributions from QCD are relatively small, they give rise to the main theoretical uncertainties, since they cannot be calculated from first principles but rely either on data-driven calculations or lattice QCD evaluations [54].

The muon $g-2$ experiment at the Fermi National Accelerator Laboratory (FNAL) [55] has recently measured the anomalous magnetic moment of the muon, updating the results from the E821 experiment at Brookhaven National Laboratory (BNL) [52], obtained in 2004. The combined experimental average of both experiments finds a deviation from the SM expectation[†] of

$$\Delta a_\mu = a_\mu^{\text{exp}} - a_\mu^{\text{SM}} = (251 \pm 59) \times 10^{-11}, \tag{1.47}$$

which is quantified to have a significance of 4.2σ [55]. These results strongly hint at the existence of new physics beyond the SM.

[†] The SM value of a_μ adopted in Ref. [55] relies on the data-driven evaluation of the hadronic contributions using e^+e^- collider data, recommended by the muon $g-2$ theory initiative [54].

In many supersymmetric models, the measured deviation in a_μ can easily be accommodated through additional Feynman diagrams involving the supersymmetric partners of the muon, the muon neutrino and the electroweak gauge bosons [56, 57]. Two exemplary lowest-order diagrams involving supersymmetric particles (introduced in section 1.2.5) are shown in figs. 1.7(b) and 1.7(c).

1.2.2 Supersymmetric Algebra

The Coleman–Mandula no-go theorem [58] dictates that the symmetry group generating a consistent spacetime QFT must be the direct product of the internal symmetry group with the Poincaré group, which in principle rules out the possibility for SUSY. The Coleman–Mandula proof, however, assumes the new symmetry to be generated by bosonic integer spin generators. The Haag–Lopuszanski–Sohnius extension [59] showed that the only possible way of non-trivially combining internal and spacetime symmetry groups is to use a Lie superalgebra and fermionic spin-1/2 generators.

A generator of supersymmetric transformations is thus an anti-commuting spinor Q that turns fermionic states $|f\rangle$ into bosonic states $|b\rangle$ and vice-versa,

$$Q\,|f\rangle = |b\rangle\,, \qquad\qquad Q\,|b\rangle = |f\rangle\,. \tag{1.48}$$

As spinors are complex objects, $Q^\dagger$ is also a symmetry operator. In order to obey the Haag–Lopuszanski–Sohnius loophole of the Coleman–Mandula theorem, both Q and $Q^\dagger$ are necessarily fermionic and thus must carry half-integer spin, meaning that SUSY must be a spacetime symmetry, i.e. a Poincaré symmetry. To simultaneously allow for parity-violating interactions, the SUSY generators have to satisfy the following algebra of commutation and anti-commutation relations [6],

$$\begin{aligned} \{Q, Q^\dagger\} &= 2\sigma_\mu P^\mu, \\ \{Q, Q\} &= \{Q^\dagger, Q^\dagger\} = 0, \\ [P^\mu, Q] &= \left[P^\mu, Q^\dagger\right] = 0, \\ \{M^{\mu\nu}, Q\} &= \sigma^{\mu\nu} Q, \\ \{M^{\mu\nu}, Q^\dagger\} &= \bar{\sigma}^{\mu\nu} Q^\dagger, \end{aligned} \tag{1.49}$$

where P^μ is the four-momentum generator of spacetime translations, $\sigma_\mu = (\mathbb{1}_2, \sigma_i)$, $\bar{\sigma}_\mu = (\mathbb{1}_2, -\sigma_i)$ with $i = 1, 2, 3$ and the Pauli matrices σ_i, and $\sigma^{\mu\nu} = \frac{i}{4}(\sigma^\mu \bar{\sigma}^\nu - \sigma^\nu \bar{\sigma}^\mu)$ as well as $\bar{\sigma}^{\mu\nu} = \frac{i}{4}(\bar{\sigma}^\mu \sigma^\nu - \bar{\sigma}^\nu \sigma^\mu)$. This is the simplest version of SUSY, called $\mathcal{N} = 1$ symmetry, as it introduces only one pair of generators. Supersymmetric theories with $\mathcal{N} \geq 2$ pairs of generators also exist and generally have some theoretical advantages as, e.g., fewer divergencies in the case of $\mathcal{N} = 2$, or even no divergencies at all in the case of $\mathcal{N} = 4$ [6]. SUSY models with $\mathcal{N} \geq 2$, however, do not allow for parity violation and thus fail to describe the physics of the SM, disqualifying them from a phenomenological point of view [6].

As both SUSY generators commute with spacetime translations (see eq. (1.49)), they also both commute with the squared mass operator $-P^2$. Consequently, particles related by the generators, called *superpartners*, must have equal eigenvalues under $-P^2$, i.e. they must have equal masses. Furthermore, the SUSY generators also commute with the gauge transformation generators, hence superpartners must have same electric charge, weak isospin and degrees of freedom in colour space [5].

1.2.3 Supermultiplets

The SM and SUSY particles are arranged in irreducible representations of the SUSY algebra, called *supermultiplets*, each containing both fermionic and bosonic states that are superpartners of each other. It can be shown that each supermultiplet has an equal number of fermion and boson degrees of freedom, $n_f = n_b$ [5].

The simplest supermultiplet Ψ that can be constructed contains a single Weyl fermion ψ and two real scalars, described by a single complex field ϕ, called the *sfermion*. The Weyl fermion has two spin helicity states, hence $n_f = 2$, and the complex scalar field has two components with $n_b = 1$ each. An additional complex scalar field F, called *auxiliary field* and not corresponding to a physical particle, has to be introduced in order to allow the SUSY algebra to close off-shell[†], where the energy-momentum relation does not hold [5]. The supermultiplet Ψ thus reads

$$\Psi = (\phi, \psi, F). \tag{1.50}$$

Being a pure bookkeeping device, the auxiliary field does not propagate and can be eliminated on-shell with the equations of motion $F = F^* = 0$. This supermultiplet is called a *chiral* or *scalar* supermultiplet [5].

The next-simplest supermultiplet for which $n_f = n_b$ holds, is the *vector* or *gauge* supermultiplet Φ containing a spin-1 gauge boson A_a^μ, where a is the index of the gauge group. In order for the theory to be renormalisable, this gauge boson must be massless before spontaneous breaking of the symmetry. As a massless spin-1 boson has two helicity states, i.e. $n_b = 2$, the superpartner, called *gaugino*, must be a massless spin-1/2 Weyl fermion λ_a with two helicity states such that $n_f = 2$ [5]. An auxiliary real bosonic field D_a is needed to balance the degrees of freedom off-shell [6], completing the supermultiplet to be

$$\Phi = (\lambda_a, A_a^\mu, D_a). \tag{1.51}$$

Like the chiral auxiliary field, the gauge auxiliary field does not correspond to a physical particle and can be eliminated on-shell through its equations of motion [5].

1.2.4 Supersymmetric Lagrangian

The simplest supersymmetric model that can be shown to realise the superalgebra is the massless, non-interacting Wess–Zumino model [60] with the action [6, 5]

$$\begin{aligned} S &= \int \mathrm{d}^4x (\mathcal{L}_{\text{scalar}} + \mathcal{L}_{\text{fermion}}), \\ \mathcal{L}_{\text{scalar}} &= -\partial^\mu \phi^* \partial_\mu \phi, \\ \mathcal{L}_{\text{fermion}} &= -i\psi^\dagger \bar{\sigma}^\mu \partial_\mu \psi, \end{aligned} \tag{1.52}$$

[†] Henceforth, the term *on-shell* describes fields that obey the equations of motion and correspond to real particles, while the term *off-shell* refers to fields that do not obey the equations of motion and correspond to virtual particles. Often, the term *off-shell* is used in an inclusive fashion, i.e. to designate particles that can also be on the mass-shell, but do not necessarily have to be.

with a massless complex scalar ϕ and a spin-1/2 fermion ψ, corresponding to a single chiral supermultiplet. As discussed in section 1.2.3, in order for this Lagrangian to satisfy the supersymmetry off-shell where the equations of motion cannot be used, an auxiliary complex scalar field F has to be added. The free Lagrangian [6] in the action thus reads

$$\mathcal{L}_{\text{free}} = \mathcal{L}_{\text{scalar}} + \mathcal{L}_{\text{fermion}} + \mathcal{L}_{\text{aux}}, \qquad \text{with} \quad \mathcal{L}_{\text{aux}} = F^{*i} F_i. \tag{1.53}$$

The auxiliary term $\mathcal{L}_{\text{aux}}$ implies the trivial equations of motion $F = F^* = 0$, which are needed to remove the auxiliary field in the on-shell case. The next step involves adding terms for non-gauge interactions for the chiral supermultiplets. Non-gauge interactions for chiral supermultiplets at most quadratic in the fermion fields can be achieved by introducing the term [6],

$$\mathcal{L}_{\text{int}} = -\frac{1}{2} W^{ij}(\phi, \phi^*)\psi_i \psi_j + V(\phi, \phi^*) + c.c., \tag{1.54}$$

where W^{ij} is a holomorphic[†] function of the complex scalar fields ϕ_i of the form [6]

$$W^{ij} = \frac{\partial^2 W}{\partial \phi_i \partial \phi_j}. \tag{1.55}$$

Here, W is called the *superpotential*. For the final Lagrangian to be renormalisable, the superpotential can at most be cubic [6], and thus can be written as

$$W = \frac{1}{2} m^{ij} \phi_i \phi_j + \frac{1}{6} y^{ijk} \phi_i \phi_j \phi_k, \tag{1.56}$$

where y^{ij} are the Yukawa couplings between the scalar and the two fermions, thus containing all non-gauge interactions. The term quadratic in the fields contains the fermion mass matrix m^{ij}, which is equal to the mass matrix of the scalar bosons due to supersymmetry, as will be shown below. Requiring $\mathcal{L}_{\text{int}}$ to be invariant under supersymmetry transformations further defines the potential V. The equations of motion of the auxiliary fields F can be written as

$$F_i = -\frac{\partial W(\phi)}{\partial \phi^i} = -W_i^*, \qquad F^{*i} = -\frac{\partial W(\phi)}{\partial \phi_i} = -W^i, \tag{1.57}$$

which thus yields for the potential $V = W_i^* W^i = F_i F^{*i}$, allowing to write the Lagrangian without explicitly introducing the auxiliary fields. The full Lagrangian of the Wess-Zumino model, with general chiral interactions between the scalar and fermion fields in the chiral supermultiplets [6], is then given by

$$\mathcal{L} = -\partial^\mu \phi^{*i} \partial_\mu \phi_i - i\psi^{\dagger i} \bar{\sigma}^\mu \partial_\mu \psi_i - \frac{1}{2} m^{ij} \psi_i \psi_j - \frac{1}{2} m^*_{ij} \psi^{\dagger i} \psi^{\dagger j} - \frac{1}{2} y^{ijk} \phi_i \psi_j \psi_k - \frac{1}{2} y^*_{ijk} \phi^{*i} \psi^{\dagger j} \psi^{\dagger k} - V(\phi, \phi^*), \tag{1.58}$$

obtained by adding the interaction term $\mathcal{L}_{\text{int}}$ from eq. (1.54) to the free Lagrangian in eq. (1.52) and inserting the expression for the superpotential from eq. (1.56) and the auxiliary fields from eq. (1.57).

The Lagrangian in eq. (1.58) immediately reveals that, as expected by supersymmetry, the masses of the fermions and bosons in the same supermultiplet are identical. In order to incorporate gauge

[†] A holomorphic function is a complex-valued function in one or more complex variables that is complex differentiable in a neighbourhood for every point of its domain.

supermultiplets and consider the interactions between fermions and gauge bosons observed in the SM, the usual minimal coupling rule has to be applied, replacing ∂_μ with D_μ. This leads to equations of motion for the auxiliary fields,

$$D^a = -g(\phi^* T^a \phi), \tag{1.59}$$

where T^a are the generators of the gauge group and g is the coupling constant [6]. The potential then becomes

$$V(\phi, \phi^*) = F^{*i} F_i + \frac{1}{2} \sum_a D^a D^a = W_i^* W^i + \frac{1}{2} \sum_a g_a^2 (\phi^* T^a \phi)^2, \tag{1.60}$$

where a runs over the gauge groups that generally have differing gauge couplings [6].

1.2.5 The Minimal Supersymmetric Standard Model

The Minimal Supersymmetric Standard Model (MSSM) is the simplest $\mathcal{N} = 1$ supersymmetric extension of the SM in the sense that it introduces a minimal set of additional particles.

Particle content and interactions

The MSSM arranges all SM particles in chiral (all the fermions and quarks) and gauge (all spin-1 bosons) supermultiplets. As supersymmetric partners have the same quantum numbers apart from spin, none of the SM particles can be superpartners of each other. Thus, all supersymmetric partners have to be new, unseen particles. Table 1.3 summaries the names, notations and spins of all superpartners introduced in the MSSM. The naming convention is to prepend the names of the superpartners of fermions with an 's' (e.g. *selectron*, *stop*, ...) and append '-ino' to the names of the superpartners of the bosons (e.g. *Wino*, *Higgsino*, ...). Supersymmetric particles (*sparticles*) are generally denoted by adding a tilde to the symbol of SM particles (e.g. $\tilde{e}$, $\tilde{u}$, $\tilde{g}$).

An important detail to note is that right-handed and left-handed fermions get their own chiral supermultiplets and thus have distinct superpartners, as otherwise the preference of the weak interaction for left-handed particles would be violated. For example, left-handed and right-handed quarks (q_L, q_R) get two different superpartners ($\tilde{q}_\mathrm{L}$, $\tilde{q}_\mathrm{R}$), denoted with subscript 'L' and 'R'. The index here refers to the handiness of the SM particle as scalar particles have only one helicity state. Additionally, the superpartners of the left-handed and right-handed fermions will mix to form physical mass eigenstates.

It is also worth asking why the superpartners of SM particles are of lower spin in the first place, as e.g. spin-1 superpartners of the SM fermions could also have been considered. The introduction of spin-1 bosons would entail the introduction of new gauge interactions, rendering the MSSM non-minimal [6]. Furthermore, introducing superpartners with spin greater than 1 would make the resulting theory non-renormalisable [6].

In the MSSM, two Higgs doublets are needed in order to give masses to the up-type and down-type quarks via Yukawa couplings. A single Higgs field h cannot be used for this as it would require Yukawa terms including the complex conjugate h^*, which is forbidden as the superpotential, being a holomorphic function of the fields, cannot depend on the complex conjugates of the same fields [6]. Additionally, the use of a single Higgs doublet would lead to gauge anomalies in the electroweak gauge symmetry [61]. Instead two complex Higgs doublets with hypercharge $Y = \pm 1/2$ are used in

Table 1.3: Particle content of the MSSM. The spin refers to the spin of the superpartner. Adapted from [6].

Particle	superpartner 0	Spin
quarks q	squarks $\tilde{q}$	0
$\rightarrow$ top t	stop $\tilde{t}$	
$\rightarrow$ bottom t	sbottom $\tilde{b}$	
...		
leptons ℓ	sleptons $\tilde{\ell}$	0
$\rightarrow$ electron e	selectron $\tilde{e}$	
$\rightarrow$ muon μ	smuon $\tilde{\mu}$	
$\rightarrow$ tau τ	stau $\tilde{\tau}$	
$\rightarrow$ neutrinos ν_ℓ	stop $\tilde{\nu}_\ell$	
gauge bosons	gauginos	1/2
$\rightarrow$ photon γ	photino $\tilde{\gamma}$	
$\rightarrow$ boson Z	Zino $\tilde{Z}$	
$\rightarrow$ boson B	Bino $\tilde{B}$	
$\rightarrow$ boson W	Wino $\tilde{W}$	
$\rightarrow$ gluon g	gluino $\tilde{g}$	
Higgs bosons $H_i^{\pm,0}$	higgsinos $\tilde{H}_i^{\pm,0}$	1/2

the MSSM. The two Higgs doublets can be written as

$$H_u = \begin{pmatrix} H_u^0 \\ H_u^- \end{pmatrix}, \qquad H_d = \begin{pmatrix} H_d^+ \\ H_d^0 \end{pmatrix}. \tag{1.61}$$

As illustrated in section 1.2.4 using the Wess–Zumino model, interactions are introduced using the superpotential. In the MSSM, the superpotential reads

$$W_{\text{MSSM}} = \bar{u}\boldsymbol{y_u}QH_u - \bar{d}\boldsymbol{y_d}QH_d - \bar{e}\boldsymbol{y_e}LH_d + \mu H_u H_d, \tag{1.62}$$

where Q and L correspond to the supermultiplets containing the left-handed quarks and leptons as well as their superpartners, respectively. Likewise, $\bar{u}$, $\bar{d}$, $\bar{e}$ correspond to the supermultiplets containing the right-handed up-type quarks, down-type quarks and leptons as well as their superpartners, respectively. The parameters $\boldsymbol{y_u}$, $\boldsymbol{y_d}$ and $\boldsymbol{y_e}$ are the 3×3 Yukawa coupling matrices. Except for the third generation, the Yukawa couplings are known to be relatively small [5] and are thus not of direct interest for the phenomenology of the theory. Phenomenologically more interesting are the supersymmetric gauge interactions that dominate the production and decay process of superpartners in the MSSM [5]. The superpotential in eq. (1.62) illustrates again why two Higgs doublets are needed in the MSSM, since terms like $\bar{u}QH_d^*$ or $\bar{e}LH_u^*$ are not allowed due to the holomorphism of the superpotential. The term $\mu H_u H_d$ contains the *higgsino mass parameter* μ and is the supersymmetric version of the Higgs mass term in the SM Lagrangian.

Soft supersymmetry breaking

As stated in section 1.2.2, all superpartners must have the same quantum numbers apart from their spin. They especially also should have the same masses. As such particles would have been discovered a

long time ago, SUSY must be a broken symmetry. If broken SUSY is, however, still to provide a solution to the Hierarchy problem, i.e. cancel the quadratic divergencies in the loop corrections to the Higgs mass parameter, then the relations between the dimensionless couplings of the SM particles and their superpartners have to be maintained [5]. Hence, only symmetry breaking terms with positive mass dimension are allowed in the Lagrangian, especially also forbidding the presence of dimensionless SUSY-breaking couplings [5]. Such a breaking of SUSY is called *soft* breaking and can be written as

$$\mathcal{L} = \mathcal{L}_{\text{SUSY}} + \mathcal{L}_{\text{soft}}, \tag{1.63}$$

where $\mathcal{L}_{\text{soft}}$ contains all the symmetry breaking terms, whilst $\mathcal{L}_{\text{SUSY}}$ is the SUSY invariant Lagrangian with all the gauge and Yukawa interactions. In a softly broken SUSY, the loop corrections to the Higgs mass parameter depend quadratically on the largest mass scale associated with the soft terms (m_{soft}). As the fine-tuning problem reappears if m_{soft} becomes too large, superpartners with masses not too far above the TeV scale are generally assumed [5].

A total of 105 new parameters with no counterpart in the SM are introduced through $\mathcal{L}_{\text{soft}}$ [5, 62]:

- Wino, bino and gluino mass parameters M_1, M_2 and M_3.
- Trilinear scalar couplings, parametrised by 3×3 matrices in generation space $\boldsymbol{a_u}$, $\boldsymbol{a_d}$, $\boldsymbol{a_e}$, representing Higgs-squark-squark and Higgs-slepton-slepton interactions.
- Hermitian 3×3 matrices in generation space $\boldsymbol{m}^2_{\boldsymbol{Q}}$, $\boldsymbol{m}^2_{\tilde{\boldsymbol{u}}}$, $\boldsymbol{m}^2_{\tilde{\boldsymbol{d}}}$, $\boldsymbol{m}^2_{\boldsymbol{L}}$, $\boldsymbol{m}^2_{\tilde{\boldsymbol{e}}}$ that represent the sfermion masses.
- SUSY breaking parameters contributing to the Higgs potential $m^2_{H_u}$, $m^2_{H_d}$ and b.

The sfermion mass matrices and the trilinear scalar couplings may introduce additional flavour mixing and CP violation, both of which are heavily constrained by experimental results. Flavour mixing in the lepton sector is for example constrained by an upper limit on $\text{BR}(\mu \rightarrow e\gamma) < 4.2 \times 10^{-12}$ [63]. Bounds on additional CP violation as well as squark mixing terms come from measurements of the electron and neutron electric moments and neutral meson systems [9]. Formally, in order to avoid these terms, SUSY breaking can be assumed to be *flavour-blind*, meaning that the mass matrices are approximately diagonal. The large Yukawa couplings for the third generation squarks and sfermions can then be achieved by assuming that the trilinear scalar couplings are proportional to the corresponding Yukawa coupling matrix [5].

As most of the parameters in the MSSM are related to soft SUSY breaking, it is not surprising that the phenomenology of the MSSM strongly depends on the exact breaking mechanism. The breaking is usually assumed to happen in a *hidden sector* and the effects of the breaking are then typically mediated by messenger fields from the hidden sector to the *visible sector* containing all the particles of the MSSM. Since the hidden sector is assumed to be only weakly or indirectly coupled to the visible sector, the phenomenology mostly depends on the mechanism mediating the breaking. The two most popular mechanisms are *gravity-mediated* and *gauge-mediated* SUSY breaking.

Mediating SUSY breaking through gravity is an attractive approach, since all particles share gravitational interactions. This makes it easy to imagine gravitational effects to be the only connection between the hidden and the visible sectors. In such models, SUSY breaking is mediated through effects of gravitational strength, suppressed by inverse powers of the Planck mass [9]. The mass of the gravitino—the superpartner of the hypothetical mediator particle of gravity, called *graviton*—is

typically of electroweak scale [64, 65]. Due to its couplings of gravitational strengths, it usually does not play a role in collider physics [9].

In gauge-mediated SUSY breaking (GMSB), additional messenger fields sharing gauge interactions with the MSSM fields are transmitting the breaking from the hidden to the visible sector. In such models, the gravitino is typically the lightest supersymmetric particle (LSP), as its mass ranges from a few eV to a few GeV, making it a candidate for DM [66].

Mass spectrum

Electroweak symmetry breaking in the MSSM is generalised to the two Higgs doublets introduced in eq. (1.61). In total, the two doublets have eight degrees of freedom, three of which are used to give masses to the $W^\pm$ and Z bosons during the breaking of $SU(2)_\mathrm{L} \otimes U(1)_Y$ to $U(1)_\mathrm{em}$ (see section 1.1.2). Thus, five physical Higgs bosons appear in the MSSM; two neutral Higgs bosons even under CP transformation, called h^0 and H^0, one neutral Higgs boson odd under CP transformation, called A^0, and finally two charged Higgs bosons, called $H^\pm$. The two Higgs doublets H_u and H_d each get a VEV (v_u and v_d, respectively) that are connected to the VEV v of the SM Higgs field by

$$v_u^2 + v_d^2 = v^2. \tag{1.64}$$

Phenomenologically, the ratio of the two VEVs is usually considered, conventionally called $\tan\beta$,

$$\tan\beta = \frac{v_u}{v_d}. \tag{1.65}$$

Due to electroweak symmetry breaking, the gauginos and higgsinos are not mass eigenstates but mix to form *electroweakinos*:

- The two charged higgsinos mix with the two charged winos to form two charged mass eigenstates $\tilde{\chi}_1^\pm$, $\tilde{\chi}_2^\pm$, called *charginos*.
- The remaining neutral higgsinos mix with the bino and neutral wino to form four neutral mass eigenstates $\tilde{\chi}_1^0$, $\tilde{\chi}_2^0$, $\tilde{\chi}_3^0$, $\tilde{\chi}_4^0$, called *neutralinos*.

Both charginos and neutralinos are by convention labeled in ascending mass order. As the exact diagonalised forms of their mass mixing matrices are, in general, relatively complicated [67], they are typically evaluated in limits where one component dominates. Neutralinos with a dominant wino, bino or higgsino component will be called wino-, bino- or higgsino-like, respectively, in the following. Likewise, charginos will be called wino- or higgsino-like, if the respective component dominates.

Squarks and sleptons also mix, respectively. As in principle any scalars with the same electric charge, colour charge and R-parity (see section 1.2.5) can mix with each other, the mass eigenstates of the sleptons and squarks should a priori be obtained through diagonalisation of three 6×6 mixing matrices (one for up-type squarks, one for down-type squarks and one for charged sleptons) and one 3×3 matrix (for sneutrinos). The assumption of flavour-blind soft SUSY breaking terms leads to most of the mixing angles being very small. As opposed to the first and second generation, the third generation sfermions have relatively large Yukawa couplings, therefore the superpartners of the left- and right-handed fermions mix to mass eigenstates $(\tilde{t}_1, \tilde{t}_2)$, $(\tilde{b}_1, \tilde{b}_2)$, $(\tilde{\tau}_1, \tilde{\tau}_2)$, again labeled in ascending mass order. The

first and second generation sfermions, on the other hand, having very small Yukawa couplings, end up in nearly mass-degenerate, unmixed pairs.

The gluino, being the only colour octet fermion of the unbroken $SU(3)_C$ gauge group, cannot mix with another fermion and is thus a mass eigenstate with mass $m_{\tilde{g}} = |M_3|$ at tree level [5, 53].

R-parity

The superpotential of the MSSM in principle allows additional gauge-invariant terms that are holomorphic in the chiral superfields but violate either lepton number (L) or baryon number (B). However, L- or B-violating processes have not been observed. Also, the L- and B-violating terms would cause a finite lifetime of the proton by allowing for it to decay, e.g., via $p \rightarrow e^+\pi^0$, a process that is heavily constrained to have a lifetime longer than 1.6×10^{34} years [68], as found by the Super-Kamiokande experiment.

In order to avoid these terms, a new symmetry, called *R-parity*, is introduced. R-parity is a multiplicatively conserved quantum number defined to be

$$P_{\mathrm{R}} = (-1)^{3(B-L)+2s}, \tag{1.66}$$

where s is the spin of the particle. Given this definition, all SM particles and the Higgs bosons have even R-parity ($P_{\mathrm{R}} = +1$) while all superpartners have odd R-parity ($P_{\mathrm{R}} = -1$). Assuming R-parity to be exactly conserved at each vertex in the MSSM leads to a number of interesting phenomenological consequences:

- Sparticles are always produced in pairs.
- Heavier sparticles decay into lighter ones.
- The number of sparticles at each vertex must be even.
- The LSP must be stable as it cannot decay any further without violating R-parity.

The nature of the LSP can be further constrained by cosmological observations [69]. If it were electrically charged or coupled to the strong interaction, it would have dissipated its energy and mixed with ordinary matter in the galactic disks, where it would have formed anomalous heavy isotopes. Upper limits on such supersymmetric relics [70] heavily favour an electrically neutral and at most weakly interacting LSP. This excludes in particular the gluino as an LSP. Another possible LSP, the sneutrino, is ruled out by Large Electron Positron (LEP) and direct searches [71–73]. Gauge-mediated supersymmetric theories often predict a light gravitino LSP with a mass ranging from a few eV to a few GeV. Another promising option, and the one considered in the following, is a neutralino LSP. In large portions of the MSSM parameter space, a neutralino LSP produces a DM relic density that is compatible with the DM relic density measured by Planck [49, 70].

Although both R-parity conserving and R-parity violating models exist and are searched for in ATLAS, for the phenomenological reasons explained above, only R-parity conserving SUSY models with neutralino LSPs are considered in the following.

Table 1.4: Parameters of the phenomenological Minimal Supersymmetric Standard Model (pMSSM).

Parameter	Meaning
$\tan\beta$	ratio of the Higgs doublet VEVs
M_A	mass of the CP-odd Higgs boson
μ	Higgs-higgsino mass parameters
M_1, M_2, M_3	wino, bino and gluino mass parameters
$m_{\tilde{q}}$, $m_{\tilde{u}_R}$, $m_{\tilde{d}_R}$, $m_{\tilde{\ell}}$, $m_{\tilde{e}_R}$	first and second generation sfermion masses
$m_{\tilde{Q}}$, $m_{\tilde{t}_R}$, $m_{\tilde{b}_R}$, $m_{\tilde{L}}$, $m_{\tilde{\tau}_R}$	third generation sfermion masses
A_t, A_b, A_τ	third generation trilinear couplings

1.2.6 The phenomenological MSSM

In addition to the 19 parameters of the SM, the MSSM adds a total of 105 additional parameters, too much to allow for a full exploration of the MSSM in experimental analyses. However, as discussed in section 1.2.5, not all values of the 105 additional parameters lead to phenomenologically viable models. By requiring a set of phenomenological constraints, the 105 free parameters can be reduced to only 19 free parameters, spanning a model space called the pMSSM [74, 75]. The free parameters in the pMSSM are listed in table 1.4.

The reduction of free parameters is obtained by applying the following constraints on the MSSM:

- No new source of CP violation, as discussed in section 1.2.5, achieved by assuming all soft breaking parameters to be real.
- Minimal flavour violation, meaning that flavour-changing neutral currents (FCNCs), heavily constrained by experiment, are not allowed and the flavour physics is governed by the CKM matrix.
- First and second sfermion generations are mass-degenerate.
- The trilinear couplings and Yukawa couplings are negligible for the first and second sfermion generations.

The pMSSM does not make any assumptions on the physics above the TeV scale, and therefore does not assume a specific SUSY breaking mechanism. With its 19 free parameters, and the typical complexity of a search for SUSY, the pMSSM is still computationally extremely challenging to probe. Using appropriate approximations, the computational complexity can be simplified enough for exhaustive scans and comparisons to experimental data to become possible. Two such approximations are discussed in chapters 9 and 10, respectively, and applied on the pMSSM in chapter 11.

1.2.7 Simplified models

In searches for BSM physics at the Large Hadron Collider (LHC), it is common to use simplified models [76–78] as a way of reducing the available parameter space to a manageable level. Simplified models do not aim to represent complete supersymmetric models but are mostly defined by a single (or a few selected) decay chain(s) allowing only a small number of participating sparticles, usually only

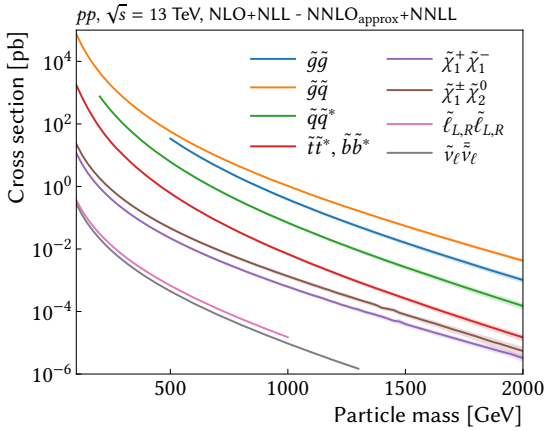

Figure 1.8: Cross sections of different SUSY production processes at $\sqrt{s} = 13\,\text{TeV}$ in pp collisions. Cross sections for pair production of electroweakinos are significantly smaller than, e.g., those for pair production of gluinos. The shaded bands correspond to the theory uncertainty of each cross section. Cross sections taken for coloured and electroweak sector taken from Refs. [81, 82] and Refs. [83–85], respectively.

two or three. Other sparticles are decoupled by setting their masses to be kinematically inaccessible at current collider experiments. The decay chains of the participating sparticles are determined by fixed branching ratios, often set to be 100%. Experimental bounds from non-observation of a given model are then typically presented in function of the physical masses of the sparticles involved in the decay chain. The model space spanned by the free parameters of the simplified model is typically called a *signal grid*, as each set of distinct mass parameter values, called *signal point*, occupies a single discrete point in this space. Figure 1.10(b) illustrates the signal grid used in part II of this thesis. The exact details of the signal grid are further discussed in section 1.3.2.

Simplified models have the inherent advantage that they circumvent the issue of having to search for SUSY in a vast parameter space where many of the parameters may only have small effects on observables. Their interpretation in terms of limits on individual SUSY production and decay topologies in function of sparticle masses is straightforward and very convenient. The hope is, that simplified models are a reasonable approximation of sizeable regions of parameter space of the more complete model they are embedded in [9]. The obvious downside is, however, that the limits obtained in simplified models are not automatically a good approximation of the true underlying constraint on the respective model parameter when interpreted in more complete SUSY models. Often, the constraints set on sparticle masses in simplified models, significantly overestimate the true constraints obtained in more complex SUSY spectra, especially when the usually assumed 100% branching fractions are no longer realised in more complete models (see e.g. [79, 80]).

One way of circumventing these issues, while sticking to the simplified model approach, is to ensure that the limits obtained in different simplified models involving different production and decay mechanisms are combined into limits representing more complex SUSY spectra. In such an approach, the simplified model limits can be seen as building blocks for more realistic SUSY models that include many different production processes and decay modes. Another possibility is to perform reinterpretations of SUSY searches—optimised for one ore more such simplified models—in more complete (and high-dimensional) SUSY model spaces, like e.g., in the pMSSM. This cannot only demonstrate the sensitivity of existing SUSY searches beyond simplified models, but also potentially identify blind spots and model regions not covered by current searches. In addition, connections to (in)direct DM searches and various SM measurements can be explored this way. Recent efforts in this direction include, e.g., Refs. [79, 86, 87]. As will be discussed in part III of this thesis, efforts reinterpreting ATLAS searches for SUSY in the pMSSM are currently ongoing. In chapter 11, a reinterpretation of the search for electroweakinos presented herein using a set of pMSSM models, is discussed.

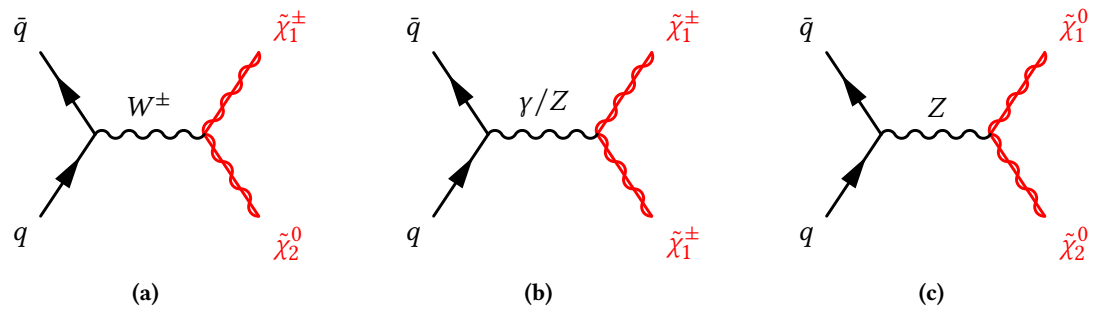

Figure 1.9: Dominant diagrams for production of electroweakino pairs at the Large Hadron Collider. Adapted from Ref. [5].

1.3 Search for electroweakinos

While both the ATLAS experiment [88] and CMS experiment [89] at the LHC at CERN set strong limits on the presence of gluinos and squarks at the TeV scale, the limits on electroweakinos are mostly still below 1 TeV. The reason for the relatively low limits on electroweakinos are the low cross-sections of electroweakino production, compared to those of squark and gluino production. As can be seen in fig. 1.8, the cross sections for $\tilde{\chi}_1^{\pm}\tilde{\chi}_2^0$ pair production (the main production process considered in the following) is more than two orders of magnitude smaller than that for gluino pair production.

Apart from the electroweakino mass limits set by the current collider experiments, some additional limits from the LEP experiments are still relevant in some corners of the phase space. Combining the results from all four LEP experiments leads to a general lower chargino mass limit of 103.5 GeV, except for scenarios with a low sneutrino mass [90]. For small mass splittings between the chargino and the LSP, the lower limit is a little weaker, with dedicated searches excluding charginos with $m(\tilde{\chi}_1^{\pm}) < 91.9\,\text{GeV}$ [90]. For mass splittings larger than 1.5 GeV and up to 50 GeV, the LEP chargino limits have recently been superseded by a dedicated ATLAS search for compressed SUSY scenarios [91], excluding chargino masses up to 240 GeV for a mass splitting of 7 GeV. For the neutralino, a lower limit on the lightest neutralino mass comes from limits on the invisible width of the Z boson, excluding $m(\tilde{\chi}_1^0) < 45.5\,\text{GeV}$, depending on the Z–neutralino coupling [9].

1.3.1 Production of electroweakinos at the Large Hadron Collider

If gluinos and squarks are heavier than a few TeV, i.e. too heavy to be within reach of the LHC, the direct production of electroweakinos might be the dominant production mode of SUSY. At hadron colliders, electroweakinos can be pair-produced directly via electroweak processes. The direct production of electroweakino pairs dominantly happens through electroweak gauge bosons from s-channel $q\bar{q}$ annihilation, as shown in fig. 1.9. Contributions from t-channels via squark exchange are typically of less importance [5].

1.3.2 Models used within this work

In SUSY scenarios where the sleptons and charged and pseudoscalar Higgs bosons are heavier than the charginos and neutralinos, a relatively pure wino lightest chargino decays predominantly through $\tilde{\chi}_1^{\pm} \rightarrow W^{\pm}\tilde{\chi}_1^0$, while the next-to-lightest neutralino decays via $\tilde{\chi}_2^0 \rightarrow Z/h\tilde{\chi}_1^0$. If, in addition, the

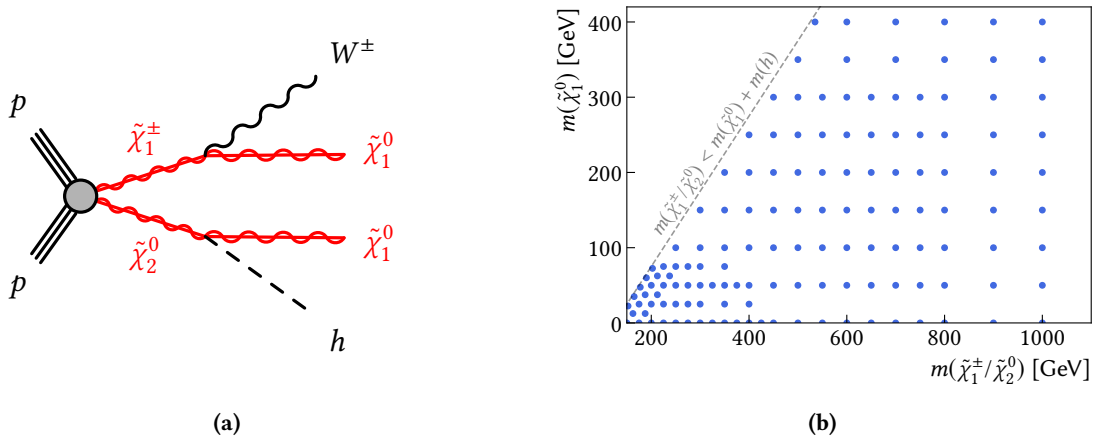

(a) (b)

Figure 1.10: Simplified model used in this thesis. Fig. (a) shows a diagram for $\tilde{\chi}_1^\pm\tilde{\chi}_2^0$ pair production with subsequent decays into $\tilde{\chi}_1^\pm \to W^\pm\tilde{\chi}_1^0$ and $\tilde{\chi}_2^0 \to h\tilde{\chi}_1^0$. Fig. (b) shows the signal grid used. Each discrete point represents a different signal model with a unique set of $\tilde{\chi}_1^\pm/\tilde{\chi}_2^0$ and $\tilde{\chi}_1^0$ mass parameters.

higgsinos are much heavier than the wino, and the mass splitting between the two lightest neutralinos is larger than the Higgs boson mass, the decay $\tilde{\chi}_2^0 \to h\tilde{\chi}_1^0$ can be the dominant decay mode of the $\tilde{\chi}_2^0$. In this case, both the $\tilde{\chi}_1^\pm$ and $\tilde{\chi}_2^0$ are wino-like and nearly mass-degenerate.

The main model used in the following is a simplified model considering direct production of a $\tilde{\chi}_1^\pm\tilde{\chi}_2^0$ pair, where the lightest chargino decays via $\tilde{\chi}_1^\pm \to W^\pm\tilde{\chi}_1^0$ and the next-to-lightest neutralino decays via $\tilde{\chi}_2^0 \to h\tilde{\chi}_1^0$, each with 100% branching ratio. The lightest chargino $\tilde{\chi}_1^\pm$ and the next-to-lightest neutralino $\tilde{\chi}_2^0$ are assumed to be degenerate in mass and pure wino states, while the lightest neutralino $\tilde{\chi}_1^0$ is considered to be a pure bino LSP. The mass parameter hierarchy for this model is thus $|M_1| < |M_2| \ll |\mu|$.

The $\tilde{\chi}_1^\pm/\tilde{\chi}_2^0$ and $\tilde{\chi}_1^0$ masses are free parameters that are systematically varied, creating a two-dimensional signal grid to be scanned and compared to data. Figure 1.10(b) shows the two-dimensional signal grid used in part II of this thesis. In the simplified model, the Higgs boson mass is set to 125 GeV in accordance with the measured value [92, 93] and its branching ratios are the ones from the SM. An exemplary diagram for the simplified model considered is shown in fig. 1.10(a).

In addition to the simplified model targeted by the SUSY search presented in the following, an additional class of models is considered in the second part of this work. These models are sampled directly from the pMSSM parameter space and are used to reinterpret the aforementioned search for direct pair production of electroweakinos. The mass spectrum of an exemplary pMSSM model point used is shown in fig. 1.11. Additional details on the sampling and phenomenology of the pMSSM models are given in chapter 11.

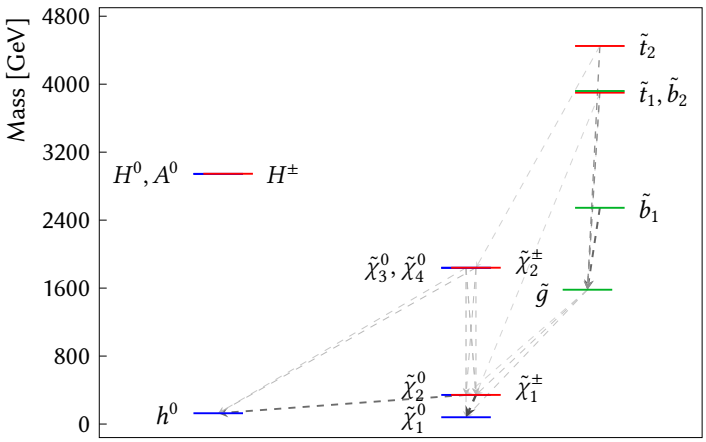

Figure 1.11: Mass spectrum of an exemplary pMSSM model. The branching fractions of the different decays are indicated through the width and and greyscale colour (black being 100%, white being 0%) of the arrows. Branching fractions smaller than 10% are suppressed for the sake of visibility. Figure generated using `pyslha` [94].

Part II

The 1-lepton analysis

Part III

Reinterpretation

Part IV

Summary and Outlook

Part V

Appendices

Abbreviations

ΛCDM Lambda Cold Dark Matter. 18

BSM beyond the Standard Model. 19, 30

CKM Cabibbo–Kobayashi–Maskawa. 6, 16, 30

CMB cosmic microwave background. 18

DM dark matter. 18, 19, 28, 29, 31

FCNC flavour-changing neutral current. 30

GUT grand unified theory. 19

LEP Large Electron Positron. 29, 32

LHC Large Hadron Collider. 30, 32

LO leading order. 8

LSP lightest supersymmetric particle. 28, 29, 32, 33

MSSM Minimal Supersymmetric Standard Model. 19, 25–30

NLO next-to-leading order. 8

PMNS Pontecorvo–Maki–Nakagawa–Sakata. 6, 16

pMSSM phenomenological Minimal Supersymmetric Standard Model. 30, 31, 33, 34

QCD quantum chromodynamics. 8, 11–13, 17, 21

QED quantum electrodynamics. 5, 8, 10–12, 14, 21

QFT quantum field theory. 7, 8, 22

SM Standard Model of particle physics. 5–8, 14–21, 23, 25, 31, 33

SUSY Supersymmetry. 17, 19, 22, 23, 27–33

VEV vacuum expectation value. 14, 16, 28, 30

WIMP weakly interacting massive particle. 18, 19

Bibliography

[1] ATLAS Collaboration, "Observation of a new particle in the search for the Standard Model Higgs boson with the ATLAS detector at the LHC," *Phys. Lett. B* **716** (2012) 1, arXiv:1207.7214 [hep-ex].

[2] CMS Collaboration, "Observation of a new boson at a mass of 125 GeV with the CMS experiment at the LHC," *Phys. Lett. B* **716** (2012) 30, arXiv:1207.7235 [hep-ex].

[3] I. C. Brock and T. Schorner-Sadenius, *Physics at the terascale*. Wiley, Weinheim, 2011. https://cds.cern.ch/record/1354959.

[4] M. E. Peskin and D. V. Schroeder, *An Introduction to quantum field theory*. Addison-Wesley, Reading, USA, 1995. http://www.slac.stanford.edu/~mpeskin/QFT.html.

[5] S. P. Martin, "A Supersymmetry primer," arXiv:hep-ph/9709356v7 [hep-ph]. [Adv. Ser. Direct. High Energy Phys.18,1(1998)].

[6] M. Bustamante, L. Cieri, and J. Ellis, "Beyond the Standard Model for Montaneros," in *5th CERN - Latin American School of High-Energy Physics*. 11, 2009. arXiv:0911.4409 [hep-ph].

[7] L. Brown, *The Birth of particle physics*. Cambridge University Press, Cambridge Cambridgeshire New York, 1986.

[8] P. J. Mohr, D. B. Newell, and B. N. Taylor, "CODATA Recommended Values of the Fundamental Physical Constants: 2014," *Rev. Mod. Phys.* **88** no. 3, (2016) 035009, arXiv:1507.07956 [physics.atom-ph].

[9] Particle Data Group, "Review of Particle Physics," *Progress of Theoretical and Experimental Physics* **2020** no. 8, (08, 2020) , https://academic.oup.com/ptep/article-pdf/2020/8/083C01/34673722/ptaa104.pdf. https://doi.org/10.1093/ptep/ptaa104. 083C01.

[10] Super-Kamiokande Collaboration, "Evidence for oscillation of atmospheric neutrinos," *Phys. Rev. Lett.* **81** (1998) 1562–1567, arXiv:hep-ex/9807003 [hep-ex].

[11] Z. Maki, M. Nakagawa, and S. Sakata, "Remarks on the unified model of elementary particles," *Prog. Theor. Phys.* **28** (1962) 870–880. [,34(1962)].

[12] N. Cabibbo, "Unitary symmetry and leptonic decays," *Phys. Rev. Lett.* **10** (Jun, 1963) 531–533. https://link.aps.org/doi/10.1103/PhysRevLett.10.531.

[13] M. Kobayashi and T. Maskawa, "CP Violation in the Renormalizable Theory of Weak Interaction," *Prog. Theor. Phys.* **49** (1973) 652–657.

[14] E. Noether and M. A. Tavel, "Invariant variation problems," arXiv:physics/0503066.

[15] J. C. Ward, "An identity in quantum electrodynamics," *Phys. Rev.* **78** (Apr, 1950) 182–182. https://link.aps.org/doi/10.1103/PhysRev.78.182.

[16] Y. Takahashi, "On the generalized ward identity," *Il Nuovo Cimento (1955-1965)* **6** no. 2, (Aug, 1957) 371–375. https://doi.org/10.1007/BF02832514.

[17] G. 'tHooft, "Renormalization of massless yang-mills fields," *Nuclear Physics B* **33** no. 1, (1971) 173 – 199. http://www.sciencedirect.com/science/article/pii/0550321371903956.

[18] J. Taylor, "Ward identities and charge renormalization of the yang-mills field," *Nuclear Physics B* **33** no. 2, (1971) 436 – 444. http://www.sciencedirect.com/science/article/pii/0550321371902975.

[19] A. A. Slavnov, "Ward identities in gauge theories," *Theoretical and Mathematical Physics* **10** no. 2, (Feb, 1972) 99–104. https://doi.org/10.1007/BF01090719.

[20] C. N. Yang and R. L. Mills, "Conservation of isotopic spin and isotopic gauge invariance," *Phys. Rev.* **96** (Oct, 1954) 191–195. https://link.aps.org/doi/10.1103/PhysRev.96.191.

[21] K. G. Wilson, "Confinement of quarks," *Phys. Rev. D* **10** (Oct, 1974) 2445–2459. https://link.aps.org/doi/10.1103/PhysRevD.10.2445.

[22] T. DeGrand and C. DeTar, *Lattice Methods for Quantum Chromodynamics*. World Scientific, Singapore, 2006. https://cds.cern.ch/record/1055545.

[23] S. L. Glashow, "Partial-symmetries of weak interactions," *Nuclear Physics* **22** no. 4, (1961) 579 – 588. http://www.sciencedirect.com/science/article/pii/0029558261904692.

[24] S. Weinberg, "A model of leptons," *Phys. Rev. Lett.* **19** (Nov, 1967) 1264–1266. https://link.aps.org/doi/10.1103/PhysRevLett.19.1264.

[25] A. Salam and J. C. Ward, "Weak and electromagnetic interactions," *Il Nuovo Cimento (1955-1965)* **11** no. 4, (Feb, 1959) 568–577. https://doi.org/10.1007/BF02726525.

[26] C. S. Wu, E. Ambler, R. W. Hayward, *et al.*, "Experimental test of parity conservation in beta decay," *Phys. Rev.* **105** (Feb, 1957) 1413–1415. https://link.aps.org/doi/10.1103/PhysRev.105.1413.

[27] M. Gell-Mann, "The interpretation of the new particles as displaced charge multiplets," *Il Nuovo Cimento (1955-1965)* **4** no. 2, (Apr, 1956) 848–866. https://doi.org/10.1007/BF02748000.

[28] K. Nishijima, "Charge Independence Theory of V Particles*," *Progress of Theoretical Physics* **13** no. 3, (03, 1955) 285–304, https://academic.oup.com/ptp/article-pdf/13/3/285/5425869/13-3-285.pdf. https://doi.org/10.1143/PTP.13.285.

[29] T. Nakano and K. Nishijima, "Charge Independence for V-particles*," *Progress of Theoretical Physics* **10** no. 5, (11, 1953) 581–582, https://academic.oup.com/ptp/article-pdf/10/5/581/5364926/10-5-581.pdf. https://doi.org/10.1143/PTP.10.581.

[30] F. Englert and R. Brout, "Broken symmetry and the mass of gauge vector mesons," *Phys. Rev. Lett.* **13** (Aug, 1964) 321–323. https://link.aps.org/doi/10.1103/PhysRevLett.13.321.

[31] P. W. Higgs, "Broken symmetries and the masses of gauge bosons," *Phys. Rev. Lett.* **13** (Oct, 1964) 508–509. https://link.aps.org/doi/10.1103/PhysRevLett.13.508.

[32] P. W. Higgs, "Spontaneous symmetry breakdown without massless bosons," *Phys. Rev.* **145** (May, 1966) 1156–1163. https://link.aps.org/doi/10.1103/PhysRev.145.1156.

[33] Y. Nambu, "Quasiparticles and Gauge Invariance in the Theory of Superconductivity," *Phys. Rev.* **117** (1960) 648–663. [,132(1960)].

[34] J. Goldstone, "Field Theories with Superconductor Solutions," *Nuovo Cim.* **19** (1961) 154–164.

[35] V. Brdar, A. J. Helmboldt, S. Iwamoto, and K. Schmitz, "Type-I Seesaw as the Common Origin of Neutrino Mass, Baryon Asymmetry, and the Electroweak Scale," *Phys. Rev. D* **100** (2019) 075029, arXiv:1905.12634 [hep-ph].

[36] G. 't Hooft and M. Veltman, "Regularization and renormalization of gauge fields," *Nuclear Physics B* **44** no. 1, (1972) 189 – 213. http://www.sciencedirect.com/science/article/pii/0550321372902799.

[37] G. L. Kane, *The supersymmetric world : the beginnings of the theory.* World Scientific, Singapore River Edge, N.J, 2000.

[38] F. Zwicky, "Die Rotverschiebung von extragalaktischen Nebeln," *Helv. Phys. Acta* **6** (1933) 110–127. https://cds.cern.ch/record/437297.

[39] V. C. Rubin and W. K. Ford, Jr., "Rotation of the Andromeda Nebula from a Spectroscopic Survey of Emission Regions," *Astrophys. J.* **159** (1970) 379–403.

[40] G. Bertone, D. Hooper, and J. Silk, "Particle dark matter: Evidence, candidates and constraints," *Phys. Rept.* **405** (2005) 279–390, arXiv:hep-ph/0404175.

[41] D. Clowe, M. Bradac, A. H. Gonzalez, *et al.*, "A direct empirical proof of the existence of dark matter," *Astrophys. J.* **648** (2006) L109–L113, arXiv:astro-ph/0608407 [astro-ph].

[42] A. Taylor, S. Dye, T. J. Broadhurst, *et al.*, "Gravitational lens magnification and the mass of abell 1689," *Astrophys. J.* **501** (1998) 539, arXiv:astro-ph/9801158.

[43] C. Bennett *et al.*, "Four year COBE DMR cosmic microwave background observations: Maps and basic results," *Astrophys. J. Lett.* **464** (1996) L1–L4, arXiv:astro-ph/9601067.

[44] G. F. Smoot *et al.*, "Structure in the COBE Differential Microwave Radiometer First-Year Maps," *ApJS* **396** (September, 1992) L1.

[45] WMAP Collaboration, "Nine-year Wilkinson Microwave Anisotropy Probe (WMAP) Observations: Final Maps and Results," *ApJS* **208** no. 2, (October, 2013) 20, arXiv:1212.5225 [astro-ph.CO].

[46] WMAP Collaboration, "Nine-year Wilkinson Microwave Anisotropy Probe (WMAP) Observations: Cosmological Parameter Results," *ApJS* **208** no. 2, (October, 2013) 19, arXiv:1212.5226 [astro-ph.CO].

[47] Planck Collaboration, "Planck 2018 results. I. Overview and the cosmological legacy of Planck," *Astron. Astrophys.* **641** (2020) A1, arXiv:1807.06205 [astro-ph.CO].

[48] A. Liddle, *An introduction to modern cosmology; 3rd ed.* Wiley, Chichester, Mar, 2015. https://cds.cern.ch/record/1976476.

[49] Planck Collaboration, "Planck 2018 results. VI. Cosmological parameters," *Astron. Astrophys.* **641** (2020) A6, arXiv:1807.06209 [astro-ph.CO].

[50] H. Georgi and S. L. Glashow, "Unity of all elementary-particle forces," *Phys. Rev. Lett.* **32** (Feb, 1974) 438–441. https://link.aps.org/doi/10.1103/PhysRevLett.32.438.

[51] I. Aitchison, *Supersymmetry in Particle Physics. An Elementary Introduction.* Cambridge University Press, Cambridge, 2007.

[52] Muon g-2 Collaboration, "Final Report of the Muon E821 Anomalous Magnetic Moment Measurement at BNL," *Phys. Rev. D* **73** (2006) 072003, arXiv:hep-ex/0602035.

[53] H. Baer and X. Tata, *Weak Scale Supersymmetry: From Superfields to Scattering Events.* Cambridge University Press, 2006.

[54] T. Aoyama *et al.*, "The anomalous magnetic moment of the muon in the Standard Model," *Phys. Rept.* **887** (2020) 1–166, arXiv:2006.04822 [hep-ph].

[55] Muon g-2 Collaboration, "Measurement of the Positive Muon Anomalous Magnetic Moment to 0.46 ppm," *Phys. Rev. Lett.* **126** no. 14, (2021) 141801, arXiv:2104.03281 [hep-ex].

[56] A. Czarnecki and W. J. Marciano, "The Muon anomalous magnetic moment: A Harbinger for 'new physics'," *Phys. Rev. D* **64** (2001) 013014, arXiv:hep-ph/0102122.

[57] J. L. Feng and K. T. Matchev, "Supersymmetry and the anomalous magnetic moment of the muon," *Phys. Rev. Lett.* **86** (2001) 3480–3483, arXiv:hep-ph/0102146.

[58] S. Coleman and J. Mandula, "All possible symmetries of the *s* matrix," *Phys. Rev.* **159** (Jul, 1967) 1251–1256. https://link.aps.org/doi/10.1103/PhysRev.159.1251.

[59] R. Haag, J. T. Lopuszanski, and M. Sohnius, "All Possible Generators of Supersymmetries of the s Matrix," *Nucl. Phys.* **B88** (1975) 257. [,257(1974)].

[60] J. Wess and B. Zumino, "Supergauge transformations in four dimensions," *Nucl. Phys. B* **70** (1974) 39.

[61] H. Georgi and S. L. Glashow, "Gauge theories without anomalies," *Phys. Rev. D* **6** (Jul, 1972) 429–431. https://link.aps.org/doi/10.1103/PhysRevD.6.429.

[62] S. Dimopoulos and D. W. Sutter, "The Supersymmetric flavor problem," *Nucl. Phys. B* **452** (1995) 496–512, arXiv:hep-ph/9504415.

[63] MEG Collaboration, T. Mori, "Final Results of the MEG Experiment," *Nuovo Cim. C* **39** no. 4, (2017) 325, arXiv:1606.08168 [hep-ex].

[64] H. P. Nilles, "Supersymmetry, Supergravity and Particle Physics," *Phys. Rept.* **110** (1984) 1–162.

[65] A. Lahanas and D. Nanopoulos, "The road to no-scale supergravity," *Physics Reports* **145** no. 1, (1987) 1 – 139. http://www.sciencedirect.com/science/article/pii/0370157387900342.

[66] J. L. Feng, A. Rajaraman, and F. Takayama, "Superweakly interacting massive particles," *Phys. Rev. Lett.* **91** (2003) 011302, arXiv:hep-ph/0302215.

[67] S. Y. Choi, J. Kalinowski, G. A. Moortgat-Pick, and P. M. Zerwas, "Analysis of the neutralino system in supersymmetric theories," *Eur. Phys. J. C* **22** (2001) 563–579, arXiv:hep-ph/0108117. [Addendum: Eur.Phys.J.C 23, 769–772 (2002)].

[68] Super-Kamiokande Collaboration, "Search for proton decay via $p \to e^+\pi^0$ and $p \to \mu^+\pi^0$ in 0.31 megaton-years exposure of the Super-Kamiokande water Cherenkov detector," *Phys. Rev.* **D95** no. 1, (2017) 012004, arXiv:1610.03597 [hep-ex].

[69] J. R. Ellis, "Beyond the standard model for hill walkers," in *1998 European School of High-Energy Physics*, pp. 133–196. 8, 1998. arXiv:hep-ph/9812235.

[70] J. R. Ellis, J. Hagelin, D. V. Nanopoulos, *et al.*, "Supersymmetric Relics from the Big Bang," *Nucl. Phys. B* **238** (1984) 453–476.

[71] D. O. Caldwell, R. M. Eisberg, D. M. Grumm, *et al.*, "Laboratory limits on galactic cold dark matter," *Phys. Rev. Lett.* **61** (Aug, 1988) 510–513. https://link.aps.org/doi/10.1103/PhysRevLett.61.510.

[72] M. Mori, M. M. Nojiri, K. S. Hirata, *et al.*, "Search for neutralino dark matter heavier than the *w* boson at kamiokande," *Phys. Rev. D* **48** (Dec, 1993) 5505–5518. https://link.aps.org/doi/10.1103/PhysRevD.48.5505.

[73] CDMS Collaboration, D. S. Akerib *et al.*, "Exclusion limits on the WIMP-nucleon cross section from the first run of the Cryogenic Dark Matter Search in the Soudan Underground Laboratory," *Phys. Rev. D* **72** (2005) 052009, arXiv:astro-ph/0507190.

[74] A. Djouadi, J.-L. Kneur, and G. Moultaka, "SuSpect: A Fortran code for the supersymmetric and Higgs particle spectrum in the MSSM," *Comput. Phys. Commun.* **176** (2007) 426–455, arXiv:hep-ph/0211331.

[75] C. F. Berger, J. S. Gainer, J. L. Hewett, and T. G. Rizzo, "Supersymmetry without prejudice," *Journal of High Energy Physics* **2009** no. 02, (Feb, 2009) 023–023. http://dx.doi.org/10.1088/1126-6708/2009/02/023.

[76] J. Alwall, P. Schuster, and N. Toro, "Simplified Models for a First Characterization of New Physics at the LHC," *Phys. Rev.* **D79** (2009) 075020, arXiv:0810.3921 [hep-ph].

[77] L. N. P. W. Group, "Simplified Models for LHC New Physics Searches," *J. Phys.* **G39** (2012) 105005, arXiv:1105.2838 [hep-ph].

[78] D. S. Alves, E. Izaguirre, and J. G. Wacker, "Where the Sidewalk Ends: Jets and Missing Energy Search Strategies for the 7 TeV LHC," *JHEP* **10** (2011) 012, arXiv:1102.5338 [hep-ph].

[79] F. Ambrogi, S. Kraml, S. Kulkarni, *et al.*, "On the coverage of the pMSSM by simplified model results," *Eur. Phys. J. C* **78** no. 3, (2018) 215, arXiv:1707.09036 [hep-ph].

[80] O. Buchmueller and J. Marrouche, "Universal mass limits on gluino and third-generation squarks in the context of Natural-like SUSY spectra," *Int. J. Mod. Phys. A* **29** no. 06, (2014) 1450032, arXiv:1304.2185 [hep-ph].

[81] W. Beenakker, C. Borschensky, M. Krämer, *et al.*, "NNLL-fast: predictions for coloured supersymmetric particle production at the LHC with threshold and Coulomb resummation," *JHEP* **12** (2016) 133, arXiv:1607.07741 [hep-ph].

[82] M. Beneke, M. Czakon, P. Falgari, *et al.*, "Threshold expansion of the $gg(q\bar{q}) \to Q\bar{Q} + X$ cross section at $\mathcal{O}(\alpha_s^4)$," *Phys. Lett. B* **690** (2010) 483, arXiv:0911.5166 [hep-ph].

[83] J. Fiaschi and M. Klasen, "Neutralino-chargino pair production at NLO+NLL with resummation-improved parton density functions for LHC Run II," *Phys. Rev. D* **98** no. 5, (2018) 055014, arXiv:1805.11322 [hep-ph].

[84] B. Fuks, M. Klasen, D. R. Lamprea, and M. Rothering, "Gaugino production in proton-proton collisions at a center-of-mass energy of 8 TeV," *JHEP* **10** (2012) 081, arXiv:1207.2159 [hep-ph].

[85] J. Fiaschi and M. Klasen, "Slepton pair production at the LHC in NLO+NLL with resummation-improved parton densities," *JHEP* **03** (2018) 094, arXiv:1801.10357 [hep-ph].

[86] ATLAS Collaboration, M. Aaboud *et al.*, "Dark matter interpretations of ATLAS searches for the electroweak production of supersymmetric particles in $\sqrt{s} = 8$ TeV proton-proton collisions," *JHEP* **09** (2016) 175, arXiv:1608.00872 [hep-ex].

[87] ATLAS Collaboration, "Summary of the ATLAS experiment's sensitivity to supersymmetry after LHC Run 1 — interpreted in the phenomenological MSSM," *JHEP* **10** (2015) 134, arXiv:1508.06608 [hep-ex].

[88] ATLAS Collaboration, "Mass reach of the atlas searches for supersymmetry." https://atlas.web.cern.ch/Atlas/GROUPS/PHYSICS/PUBNOTES/ATL-PHYS-PUB-2020-020/fig_23.png, 2020.

[89] CMS Collaboration, "Summary plot moriond 2017." https://twiki.cern.ch/twiki/pub/CMSPublic/SUSYSummary2017/Moriond2017_BarPlot.pdf, 2017.

[90] L. S. W. Group, "Notes lepsusywg/02-04.1 and lepsusywg/01-03.1." http://lepsusy.web.cern.ch/lepsusy/, 2004. Accessed: 2021-02-11.

[91] ATLAS Collaboration, "Searches for electroweak production of supersymmetric particles with compressed mass spectra in $\sqrt{s} = 13$ TeV pp collisions with the ATLAS detector," *Phys. Rev. D* **101** (2020) 052005, arXiv:1911.12606 [hep-ex].

[92] ATLAS Collaboration, "Observation of a new particle in the search for the Standard Model Higgs boson with the ATLAS detector at the LHC," *Phys. Lett. B* **716** (2012) 1–29, arXiv:1207.7214 [hep-ex].

[93] CMS Collaboration, "Observation of a New Boson at a Mass of 125 GeV with the CMS Experiment at the LHC," *Phys. Lett. B* **716** (2012) 30–61, arXiv:1207.7235 [hep-ex].

[94] A. Buckley, "PySLHA: a Pythonic interface to SUSY Les Houches Accord data," *Eur. Phys. J. C* **75** no. 10, (2015) 467, arXiv:1305.4194 [hep-ph].

[95] CERN, "About cern." https://home.cern/about. Accessed: 2021-01-21.

[96] CERN, "CERN Annual report 2019," tech. rep., CERN, Geneva, 2020. https://cds.cern.ch/record/2723123.

[97] O. S. Bruning, P. Collier, P. Lebrun, *et al.*, *LHC Design Report*. CERN Yellow Reports: Monographs. CERN, Geneva, 2004. https://cds.cern.ch/record/782076.

[98] M. Blewett and N. Vogt-Nilsen, "Proceedings of the 8th international conference on high-energy accelerators, cern 1971. conference held at geneva, 20–24 september 1971.," tech. rep., 1971, 1971.

[99] L. R. Evans and P. Bryant, "LHC Machine," *JINST* **3** (2008) S08001. 164 p. http://cds.cern.ch/record/1129806. This report is an abridged version of the LHC Design Report (CERN-2004-003).

[100] R. Scrivens, M. Kronberger, D. Küchler, *et al.*, "Overview of the status and developments on primary ion sources at CERN*,". https://cds.cern.ch/record/1382102.

[101] M. Vretenar, J. Vollaire, R. Scrivens, *et al.*, *Linac4 design report*, vol. 6 of *CERN Yellow Reports: Monographs*. CERN, Geneva, 2020. https://cds.cern.ch/record/2736208.

[102] E. Mobs, "The CERN accelerator complex - 2019. Complexe des accélérateurs du CERN - 2019,". https://cds.cern.ch/record/2684277. General Photo.

[103] ATLAS Collaboration, "The ATLAS Experiment at the CERN Large Hadron Collider," *JINST* **3** (2008) S08003.

[104] CMS Collaboration, "The CMS Experiment at the CERN LHC," *JINST* **3** (2008) S08004.

[105] ALICE Collaboration, "The ALICE experiment at the CERN LHC," *JINST* **3** (2008) S08002.

[106] LHCb Collaboration, "The LHCb Detector at the LHC," *JINST* **3** (2008) S08005.

[107] TOTEM Collaboration, "The TOTEM experiment at the CERN Large Hadron Collider," *JINST* **3** (2008) S08007.

[108] LHCf Collaboration, "Technical design report of the LHCf experiment: Measurement of photons and neutral pions in the very forward region of LHC,".

[109] MoEDAL Collaboration, "Technical Design Report of the MoEDAL Experiment,".

[110] ATLAS Collaboration, "ATLAS Public Results - Luminosity Public Results Run 2,". https://twiki.cern.ch/twiki/bin/view/AtlasPublic/LuminosityPublicResultsRun2. Accessed: 2021-01-17.

[111] ATLAS Collaboration, Z. Marshall, "Simulation of Pile-up in the ATLAS Experiment," *J. Phys. Conf. Ser.* **513** (2014) 022024.

[112] "First beam in the LHC - accelerating science,". https://home.cern/news/news/accelerators/record-luminosity-well-done-lhc. Accessed: 2021-01-10.

[113] ATLAS Collaboration, "Luminosity determination in pp collisions at $\sqrt{s}$ = 13 TeV using the ATLAS detector at the LHC," Tech. Rep. ATLAS-CONF-2019-021, CERN, Geneva, Jun, 2019. https://cds.cern.ch/record/2677054.

[114] ATLAS Collaboration, "Luminosity determination in pp collisions at $\sqrt{s}$ = 8 TeV using the ATLAS detector at the LHC," *Eur. Phys. J. C* **76** no. 12, (2016) 653, arXiv:1608.03953 [hep-ex].

[115] G. Avoni, M. Bruschi, G. Cabras, *et al.*, "The new LUCID-2 detector for luminosity measurement and monitoring in ATLAS," *Journal of Instrumentation* **13** no. 07, (Jul, 2018) P07017–P07017. https://doi.org/10.1088/1748-0221/13/07/p07017.

[116] S. van der Meer, "Calibration of the effective beam height in the ISR," Tech. Rep. CERN-ISR-PO-68-31. ISR-PO-68-31, CERN, Geneva, 1968. https://cds.cern.ch/record/296752.

[117] P. Grafström and W. Kozanecki, "Luminosity determination at proton colliders," *Progress in Particle and Nuclear Physics* **81** (2015) 97 – 148. http://www.sciencedirect.com/science/article/pii/S0146641014000878.

[118] M. Bajko *et al.*, "Report of the Task Force on the Incident of 19th September 2008 at the LHC," Tech. Rep. LHC-PROJECT-Report-1168. CERN-LHC-PROJECT-Report-1168, CERN, Geneva, Mar, 2009. https://cds.cern.ch/record/1168025.

[119] "New schedule for CERN's accelerators and experiments,". https://home.cern/news/press-release/cern/first-beam-lhc-accelerating-science. Accessed: 2021-01-10.

[120] ATLAS Collaboration, "Luminosity Determination in pp Collisions at $\sqrt{s}$ = 7 TeV Using the ATLAS Detector at the LHC," *Eur. Phys. J. C* **71** (2011) 1630, arXiv:1101.2185 [hep-ex].

[121] ATLAS Collaboration, "Improved luminosity determination in pp collisions at $\sqrt{s}$ = 7 TeV using the ATLAS detector at the LHC.," *Eur. Phys. J. C* **73** no. CERN-PH-EP-2013-026, (Feb, 2013) 2518. 27 p. https://cds.cern.ch/record/1517411.

[122] "Record luminosity: well done LHC,". https://home.cern/news/news/accelerators/new-schedule-cerns-accelerators-and-experiments. Accessed: 2021-01-10.

[123] A. G., B. A. I., B. O., *et al.*, *High-Luminosity Large Hadron Collider (HL-LHC): Technical Design Report V. 0.1*. CERN Yellow Reports: Monographs. CERN, Geneva, 2017. https://cds.cern.ch/record/2284929.

[124] J. Pequenao, "Computer generated image of the whole ATLAS detector." Mar, 2008.

[125] ATLAS Collaboration, "ATLAS: Detector and physics performance technical design report. Volume 1,".

[126] J. Pequenao, "Computer generated image of the ATLAS inner detector." Mar, 2008.

[127] ATLAS Collaboration, K. Potamianos, "The upgraded Pixel detector and the commissioning of the Inner Detector tracking of the ATLAS experiment for Run-2 at the Large Hadron Collider," Tech. Rep. ATL-PHYS-PROC-2016-104, CERN, Geneva, Aug, 2016. https://cds.cern.ch/record/2209070. 15 pages, EPS-HEP 2015 Proceedings.

[128] ATLAS IBL Collaboration, "Production and Integration of the ATLAS Insertable B-Layer," *JINST* **13** no. 05, (2018) T05008, arXiv:1803.00844 [physics.ins-det].

[129] ATLAS Collaboration, "ATLAS Insertable B-Layer Technical Design Report," Tech. Rep. CERN-LHCC-2010-013. ATLAS-TDR-19, Sep, 2010. http://cds.cern.ch/record/1291633.

[130] ATLAS Collaboration, "ATLAS b-jet identification performance and efficiency measurement with $t\bar{t}$ events in pp collisions at $\sqrt{s}$ = 13 TeV," *Eur. Phys. J. C* **79** no. 11, (2019) 970, arXiv:1907.05120 [hep-ex].

[131] ATLAS Collaboration, "Particle Identification Performance of the ATLAS Transition Radiation Tracker." ATLAS-CONF-2011-128, 2011. https://cds.cern.ch/record/1383793.

[132] J. Pequenao, "Computer Generated image of the ATLAS calorimeter." Mar, 2008.

[133] J. Pequenao, "Computer generated image of the ATLAS Muons subsystem." Mar, 2008.

[134] S. Lee, M. Livan, and R. Wigmans, "Dual-Readout Calorimetry," *Rev. Mod. Phys.* **90** no. arXiv:1712.05494. 2, (Dec, 2017) 025002. 40 p. https://cds.cern.ch/record/2637852. 44 pages, 53 figures, accepted for publication in Review of Modern Physics.

[135] M. Leite, "Performance of the ATLAS Zero Degree Calorimeter," Tech. Rep. ATL-FWD-PROC-2013-001, CERN, Geneva, Nov, 2013. https://cds.cern.ch/record/1628749.

[136] S. Abdel Khalek *et al.*, "The ALFA Roman Pot Detectors of ATLAS," *JINST* **11** no. 11, (2016) P11013, arXiv:1609.00249 [physics.ins-det].

[137] U. Amaldi, G. Cocconi, A. Diddens, *et al.*, "The real part of the forward proton proton scattering amplitude measured at the cern intersecting storage rings," *Physics Letters B* **66** no. 4, (1977) 390 – 394. http://www.sciencedirect.com/science/article/pii/0370269377900223.

[138] L. Adamczyk, E. Banaś, A. Brandt, *et al.*, "Technical Design Report for the ATLAS Forward Proton Detector," Tech. Rep. CERN-LHCC-2015-009. ATLAS-TDR-024, May, 2015. https://cds.cern.ch/record/2017378.

[139] ATLAS Collaboration, A. R. Martínez, "The Run-2 ATLAS Trigger System," *J. Phys. Conf. Ser.* **762** no. 1, (2016) 012003.

[140] ATLAS Collaboration, *ATLAS level-1 trigger: Technical Design Report.* Technical Design Report ATLAS. CERN, Geneva, 1998. https://cds.cern.ch/record/381429.

[141] ATLAS Collaboration, "Operation of the ATLAS trigger system in Run 2," *JINST* **15** no. 10, (2020) P10004, arXiv:2007.12539 [physics.ins-det].

[142] ATLAS Collaboration, P. Jenni, M. Nessi, M. Nordberg, and K. Smith, *ATLAS high-level trigger, data-acquisition and controls: Technical Design Report.* Technical Design Report ATLAS. CERN, Geneva, 2003. https://cds.cern.ch/record/616089.

[143] ATLAS Collaboration, "The ATLAS Simulation Infrastructure," *Eur. Phys. J. C* **70** (2010) 823–874, arXiv:1005.4568 [physics.ins-det].

[144] T. Gleisberg, S. Hoeche, F. Krauss, *et al.*, "Event generation with SHERPA 1.1," *JHEP* **02** (2009) 007, arXiv:0811.4622 [hep-ph].

[145] A. Buckley *et al.*, "General-purpose event generators for LHC physics," *Phys. Rept.* **504** (2011) 145–233, arXiv:1101.2599 [hep-ph].

[146] V. N. Gribov and L. N. Lipatov, "Deep inelastic e p scattering in perturbation theory," *Sov. J. Nucl. Phys.* **15** (1972) 438–450.

[147] J. Blumlein, T. Doyle, F. Hautmann, *et al.*, "Structure functions in deep inelastic scattering at HERA," in *Workshop on Future Physics at HERA (To be followed by meetings 7-9 Feb and 30-31 May 1996 at DESY)*. 9, 1996. arXiv:hep-ph/9609425.

[148] A. Buckley, J. Ferrando, S. Lloyd, *et al.*, "LHAPDF6: parton density access in the LHC precision era," *Eur. Phys. J. C* **75** (2015) 132, arXiv:1412.7420 [hep-ph].

[149] M. Bengtsson and T. Sjostrand, "Coherent Parton Showers Versus Matrix Elements: Implications of PETRA - PEP Data," *Phys. Lett. B* **185** (1987) 435.

[150] S. Catani, F. Krauss, R. Kuhn, and B. R. Webber, "QCD matrix elements + parton showers," *JHEP* **11** (2001) 063, arXiv:hep-ph/0109231.

[151] L. Lonnblad, "Correcting the color dipole cascade model with fixed order matrix elements," *JHEP* **05** (2002) 046, arXiv:hep-ph/0112284.

[152] B. Andersson, G. Gustafson, G. Ingelman, and T. Sjostrand, "Parton Fragmentation and String Dynamics," *Phys. Rept.* **97** (1983) 31–145.

[153] B. Andersson, *The Lund Model*. Cambridge Monographs on Particle Physics, Nuclear Physics and Cosmology. Cambridge University Press, 1998.

[154] D. Amati and G. Veneziano, "Preconfinement as a Property of Perturbative QCD," *Phys. Lett. B* **83** (1979) 87–92.

[155] D. Yennie, S. Frautschi, and H. Suura, "The infrared divergence phenomena and high-energy processes," *Annals of Physics* **13** no. 3, (1961) 379–452. https://www.sciencedirect.com/science/article/pii/0003491661901518.

[156] M. Dobbs and J. B. Hansen, "The HepMC C++ Monte Carlo event record for High Energy Physics," *Comput. Phys. Commun.* **134** (2001) 41–46.

[157] GEANT4 Collaboration, "GEANT4: A Simulation toolkit," *Nucl. Instrum. Meth.* **A506** (2003) 250–303.

[158] ATLAS Collaboration, "The new Fast Calorimeter Simulation in ATLAS," Tech. Rep. ATL-SOFT-PUB-2018-002, CERN, Geneva, Jul, 2018. https://cds.cern.ch/record/2630434.

[159] K. Cranmer, "Practical Statistics for the LHC," in *2011 European School of High-Energy Physics*, pp. 267–308. 2014. arXiv:1503.07622 [physics.data-an].

[160] G. Cowan, K. Cranmer, E. Gross, and O. Vitells, "Asymptotic formulae for likelihood-based tests of new physics," *Eur. Phys. J.* **C71** (2011) 1554, arXiv:1007.1727 [physics.data-an]. [Erratum: Eur. Phys. J.C73,2501(2013)].

[161] ATLAS Collaboration, "Reproduction searches for new physics with the ATLAS experiment through publication of full statistical likelihoods." ATL-PHYS-PUB-2019-029, 2019. https://cds.cern.ch/record/2684863.

[162] ROOT Collaboration, K. Cranmer, G. Lewis, L. Moneta, *et al.*, "HistFactory: A tool for creating statistical models for use with RooFit and RooStats," Tech. Rep. CERN-OPEN-2012-016, New York U., New York, Jan, 2012. https://cds.cern.ch/record/1456844.

[163] W. Verkerke and D. P. Kirkby, "The RooFit toolkit for data modeling," *eConf* **C0303241** (2003) MOLT007, arXiv:physics/0306116 [physics]. [,186(2003)].

[164] F. James and M. Roos, "MINUIT: a system for function minimization and analysis of the parameter errors and corrections," *Comput. Phys. Commun.* **10** no. CERN-DD-75-20, (Jul, 1975) 343–367. 38 p. https://cds.cern.ch/record/310399.

[165] L. Moneta, K. Belasco, K. S. Cranmer, *et al.*, "The RooStats Project," *PoS* **ACAT2010** (2010) 057, arXiv:1009.1003 [physics.data-an].

[166] R. Brun and F. Rademakers, "ROOT: An object oriented data analysis framework," *Nucl. Instrum. Meth.* **A389** (1997) 81–86.

[167] I. Antcheva *et al.*, "ROOT — A C++ framework for petabyte data storage, statistical analysis and visualization," *Computer Physics Communications* **182** no. 6, (2011) 1384 – 1385. http://www.sciencedirect.com/science/article/pii/S0010465511000701.

[168] M. Baak, G. J. Besjes, D. Côte, A. Koutsman, J. Lorenz, D. Short, "HistFitter software framework for statistical data analysis," *Eur. Phys. J.* **C75** (2015) 153, arXiv:1410.1280 [hep-ex].

[169] L. Heinrich, M. Feickert, G. Stark, and K. Cranmer, "pyhf: pure-python implementation of histfactory statistical models," *Journal of Open Source Software* **6** no. 58, (2021) 2823. https://doi.org/10.21105/joss.02823.

[170] L. Heinrich, M. Feickert, and G. Stark, "pyhf: v0.6.0," Version 0.6.0. https://github.com/scikit-hep/pyhf.

[171] C. R. Harris, K. J. Millman, S. J. van der Walt, *et al.*, "Array programming with NumPy," *Nature* **585** no. 7825, (Sept., 2020) 357–362. https://doi.org/10.1038/s41586-020-2649-2.

[172] A. Paszke, S. Gross, F. Massa, *et al.*, "Pytorch: An imperative style, high-performance deep learning library," in *Advances in Neural Information Processing Systems 32*, H. Wallach, H. Larochelle, A. Beygelzimer, *et al.*, eds., pp. 8024–8035. Curran Associates, Inc., 2019. http://papers.neurips.cc/paper/9015-pytorch-an-imperative-style-high-performance-deep-learning-library.pdf.

[173] M. Abadi, A. Agarwal, P. Barham, *et al.*, "TensorFlow: Large-scale machine learning on heterogeneous systems," 2015. https://www.tensorflow.org/. Software available from tensorflow.org.

[174] J. Bradbury, R. Frostig, P. Hawkins, *et al.*, "JAX: composable transformations of Python+NumPy programs," Version 0.1.46, 2018. http://github.com/google/jax.

[175] S. S. Wilks, "The large-sample distribution of the likelihood ratio for testing composite hypotheses," *Ann. Math. Statist.* **9** no. 1, (03, 1938) 60–62. https://doi.org/10.1214/aoms/1177732360.

[176] A. Wald, "Tests of statistical hypotheses concerning several parameters when the number of observations is large," *Transactions of the American Mathematical Society* **54** no. 3, (1943) 426–482. https://doi.org/10.1090/S0002-9947-1943-0012401-3.

[177] G. Cowan, "Statistics for Searches at the LHC," in *69th Scottish Universities Summer School in Physics: LHC Physics*, pp. 321–355. 7, 2013. arXiv:1307.2487 [hep-ex].

[178] A. L. Read, "Presentation of search results: the CL_S technique," *J. Phys. G* **28** (2002) 2693.

[179] R. D. Cousins, J. T. Linnemann, and J. Tucker, "Evaluation of three methods for calculating statistical significance when incorporating a systematic uncertainty into a test of the background-only hypothesis for a Poisson process," *Nucl. Instrum. Meth. A* **595** no. 2, (2008) 480, arXiv:physics/0702156 [physics.data-an].

[180] K. Cranmer, "Statistical challenges for searches for new physics at the LHC," in *Statistical Problems in Particle Physics, Astrophysics and Cosmology (PHYSTAT 05): Proceedings, Oxford, UK, September 12-15, 2005*, pp. 112–123. 2005. arXiv:physics/0511028 [physics.data-an]. http://www.physics.ox.ac.uk/phystat05/proceedings/files//Cranmer_LHCStatisticalChallenges.ps.

[181] ATLAS Collaboration, "Search for direct pair production of a chargino and a neutralino decaying to the 125 GeV Higgs boson in $\sqrt{s} = 8$ TeV pp collisions with the ATLAS detector," *Eur. Phys. J. C* **75** (2015) 208, arXiv:1501.07110 [hep-ex].

[182] ATLAS Collaboration, "Search for chargino and neutralino production in final states with a Higgs boson and missing transverse momentum at $\sqrt{s} = 13$ TeV with the ATLAS detector," *Phys. Rev. D* **100** (2019) 012006, arXiv:1812.09432 [hep-ex].

[183] CMS Collaboration, "Search for electroweak production of charginos and neutralinos in WH events in proton–proton collisions at $\sqrt{s} = 13$ TeV," *JHEP* **11** (2017) 029, arXiv:1706.09933 [hep-ex].

[184] ATLAS Collaboration, "Search for direct production of electroweakinos in final states with one lepton, missing transverse momentum and a Higgs boson decaying into two b-jets in pp collisions at $\sqrt{s} = 13$ TeV with the ATLAS detector," *Eur. Phys. J. C* **80** (2020) 691, arXiv:1909.09226 [hep-ex].

[185] ATLAS Collaboration, "Improvements in $t\bar{t}$ modelling using NLO+PS Monte Carlo generators for Run 2." ATL-PHYS-PUB-2018-009, 2018. https://cds.cern.ch/record/2630327.

[186] ATLAS Collaboration, "Modelling of the $t\bar{t}H$ and $t\bar{t}V(V = W, Z)$ processes for $\sqrt{s} = 13$ TeV ATLAS analyses." ATL-PHYS-PUB-2016-005, 2016. https://cds.cern.ch/record/2120826.

[187] ATLAS Collaboration, "ATLAS simulation of boson plus jets processes in Run 2." ATL-PHYS-PUB-2017-006, 2017. https://cds.cern.ch/record/2261937.

[188] ATLAS Collaboration, "Multi-Boson Simulation for 13 TeV ATLAS Analyses." ATL-PHYS-PUB-2017-005, 2017. https://cds.cern.ch/record/2261933.

[189] J. Alwall, R. Frederix, S. Frixione, *et al.*, "The automated computation of tree-level and next-to-leading order differential cross sections, and their matching to parton shower simulations," *JHEP* **07** (2014) 079, arXiv:1405.0301 [hep-ph].

[190] R. Frederix and S. Frixione, "Merging meets matching in MC@NLO," *JHEP* **12** (2012) 061, arXiv:1209.6215 [hep-ph].

[191] "Parton distributions with LHC data," *Nucl. Phys. B* **867** (2013) 244, arXiv:1207.1303 [hep-ph].

[192] T. Sjöstrand, S. Ask, J. R. Christiansen, *et al.*, "An Introduction to PYTHIA 8.2," *Comput. Phys. Commun.* **191** (2015) 159–177, arXiv:1410.3012 [hep-ph].

[193] ATLAS Collaboration, "ATLAS Pythia 8 tunes to 7 TeV data." ATL-PHYS-PUB-2014-021, 2014. https://cds.cern.ch/record/1966419.

[194] L. Lönnblad and S. Prestel, "Matching tree-level matrix elements with interleaved showers," *JHEP* **03** (2012) 019, arXiv:1109.4829 [hep-ph].

[195] D. J. Lange, "The EvtGen particle decay simulation package," *Nucl. Instrum. Meth. A* **462** (2001) 152.

[196] ATLAS Collaboration, "The Pythia 8 A3 tune description of ATLAS minimum bias and inelastic measurements incorporating the Donnachie–Landshoff diffractive model." ATL-PHYS-PUB-2016-017, 2016. https://cds.cern.ch/record/2206965.

[197] B. Fuks, M. Klasen, D. R. Lamprea, and M. Rothering, "Precision predictions for electroweak superpartner production at hadron colliders with RESUMMINO," *Eur. Phys. J. C* **73** (2013) 2480, arXiv:1304.0790 [hep-ph].

[198] S. Alioli, P. Nason, C. Oleari, and E. Re, "A general framework for implementing NLO calculations in shower Monte Carlo programs: the POWHEG BOX," *JHEP* **06** (2010) 043, arXiv:1002.2581 [hep-ph].

[199] S. Frixione, P. Nason, and G. Ridolfi, "A Positive-weight next-to-leading-order Monte Carlo for heavy flavour hadroproduction," *JHEP* **09** (2007) 126, arXiv:0707.3088 [hep-ph].

[200] P. Nason, "A New method for combining NLO QCD with shower Monte Carlo algorithms," *JHEP* **11** (2004) 040, arXiv:hep-ph/0409146.

[201] E. Bothmann *et al.*, "Event generation with Sherpa 2.2," *SciPost Phys.* **7** no. 3, (2019) 034, arXiv:1905.09127 [hep-ph].

[202] NNPDF Collaboration, "Parton distributions for the LHC run II," *JHEP* **04** (2015) 040, arXiv:1410.8849 [hep-ph].

[203] M. Czakon and A. Mitov, "Top++: A program for the calculation of the top-pair cross-section at hadron colliders," *Comput. Phys. Commun.* **185** (2014) 2930, arXiv:1112.5675 [hep-ph].

[204] M. Cacciari, M. Czakon, M. Mangano, *et al.*, "Top-pair production at hadron colliders with next-to-next-to-leading logarithmic soft-gluon resummation," *Phys. Lett. B* **710** (2012) 612–622, arXiv:1111.5869 [hep-ph].

[205] P. Kant, O. M. Kind, T. Kintscher, *et al.*, "HatHor for single top-quark production: Updated predictions and uncertainty estimates for single top-quark production in hadronic collisions," *Comput. Phys. Commun.* **191** (2015) 74–89, arXiv:1406.4403 [hep-ph].

[206] N. Kidonakis, "Two-loop soft anomalous dimensions for single top quark associated production with a W^- or H^-," *Phys. Rev. D* **82** (2010) 054018, arXiv:1005.4451 [hep-ph].

[207] J. M. Campbell and R. K. Ellis, "$t\bar{t}W^{+-}$ production and decay at NLO," *JHEP* **07** (2012) 052, arXiv:1204.5678 [hep-ph].

[208] A. Lazopoulos, T. McElmurry, K. Melnikov, and F. Petriello, "Next-to-leading order QCD corrections to $t\bar{t}Z$ production at the LHC," *Phys. Lett. B* **666** (2008) 62–65, arXiv:0804.2220 [hep-ph].

[209] R. Gavin, Y. Li, F. Petriello, and S. Quackenbush, "FEWZ 2.0: A code for hadronic Z production at next-to-next-to-leading order," arXiv:1011.3540 [hep-ph].

[210] LHC Higgs Cross Section Working Group Collaboration, "Handbook of LHC Higgs Cross Sections: 4. Deciphering the Nature of the Higgs Sector," arXiv:1610.07922 [hep-ph].

[211] ATLAS Collaboration, "Example ATLAS tunes of Pythia8, Pythia6 and Powheg to an observable sensitive to Z boson transverse momentum." ATL-PHYS-PUB-2013-017, 2013. https://cds.cern.ch/record/1629317.

[212] ATLAS Collaboration, "Performance of the ATLAS track reconstruction algorithms in dense environments in LHC Run 2," *Eur. Phys. J. C* **77** (2017) 673, arXiv:1704.07983 [hep-ex].

[213] R. Frühwirth, "Application of Kalman filtering to track and vertex fitting," *Nucl. Instrum. Methods Phys. Res., A* **262** no. HEPHY-PUB-503, (Jun, 1987) 444. 19 p. https://cds.cern.ch/record/178627.

[214] T. Cornelissen, M. Elsing, I. Gavrilenko, *et al.*, "The new ATLAS track reconstruction (NEWT)," *J. Phys.: Conf. Ser.* **119** (2008) 032014. https://cds.cern.ch/record/1176900.

[215] ATLAS Collaboration, "Vertex Reconstruction Performance of the ATLAS Detector at $\sqrt{s}$ = 13 TeV." ATL-PHYS-PUB-2015-026, 2015. https://cds.cern.ch/record/2037717.

[216] ATLAS Collaboration, "Reconstruction of primary vertices at the ATLAS experiment in Run 1 proton–proton collisions at the LHC," *Eur. Phys. J. C* **77** (2017) 332, arXiv:1611.10235 [hep-ex].

[217] ATLAS Collaboration, "Topological cell clustering in the ATLAS calorimeters and its performance in LHC Run 1," *Eur. Phys. J. C* **77** (2017) 490, arXiv:1603.02934 [hep-ex].

[218] ATLAS Collaboration, "Electron and photon performance measurements with the ATLAS detector using the 2015–2017 LHC proton–proton collision data," *JINST* **14** (2019) P12006, arXiv:1908.00005 [hep-ex].

[219] ATLAS Collaboration, "Measurement of the photon identification efficiencies with the ATLAS detector using LHC Run 2 data collected in 2015 and 2016," *Eur. Phys. J. C* **79** (2019) 205, arXiv:1810.05087 [hep-ex].

[220] ATLAS Collaboration, "Electron reconstruction and identification in the ATLAS experiment using the 2015 and 2016 LHC proton–proton collision data at $\sqrt{s}$ = 13 TeV," *Eur. Phys. J. C* **79** (2019) 639, arXiv:1902.04655 [hep-ex].

[221] ATLAS Collaboration, "Muon reconstruction performance of the ATLAS detector in proton–proton collision data at $\sqrt{s}$ = 13 TeV," *Eur. Phys. J. C* **76** (2016) 292, arXiv:1603.05598 [hep-ex].

[222] ATLAS Collaboration, "Muon reconstruction and identification efficiency in ATLAS using the full Run 2 pp collision data set at $\sqrt{s}$ = 13 TeV," arXiv:2012.00578 [hep-ex].

[223] M. Cacciari, G. P. Salam, and G. Soyez, "The anti-k_t jet clustering algorithm," *JHEP* **04** (2008) 063, arXiv:0802.1189 [hep-ph].

[224] M. Cacciari, G. P. Salam, and G. Soyez, "FastJet user manual," *Eur. Phys. J. C* **72** (2012) 1896, arXiv:1111.6097 [hep-ph].

[225] M. Cacciari, "FastJet: A Code for fast k_t clustering, and more," in *Deep inelastic scattering. Proceedings, 14th International Workshop, DIS 2006, Tsukuba, Japan, April 20-24, 2006*, pp. 487–490. 2006. arXiv:hep-ph/0607071 [hep-ph]. [,125(2006)].

[226] ATLAS Collaboration, "Jet energy scale and resolution measured in proton-proton collisions at $\sqrt{s}$ = 13 TeV with the ATLAS detector," arXiv:2007.02645 [hep-ex].

[227] M. Cacciari and G. P. Salam, "Pileup subtraction using jet areas," *Phys. Lett. B* **659** (2008) 119–126, arXiv:0707.1378 [hep-ph].

[228] ATLAS Collaboration, "Jet energy measurement with the ATLAS detector in proton–proton collisions at $\sqrt{s}$ = 7 TeV," *Eur. Phys. J. C* **73** (2013) 2304, arXiv:1112.6426 [hep-ex].

[229] ATLAS Collaboration, "Determination of jet calibration and energy resolution in proton–proton collisions at $\sqrt{s}$ = 8 TeV using the ATLAS detector," arXiv:1910.04482 [hep-ex].

[230] ATLAS Collaboration, "Performance of pile-up mitigation techniques for jets in pp collisions at $\sqrt{s}$ = 8 TeV using the ATLAS detector," *Eur. Phys. J. C* **76** (2016) 581, arXiv:1510.03823 [hep-ex].

[231] ATLAS Collaboration, "Optimisation and performance studies of the ATLAS b-tagging algorithms for the 2017-18 LHC run." ATL-PHYS-PUB-2017-013, 2017. https://cds.cern.ch/record/2273281.

[232] ATLAS Collaboration, "ATLAS b-jet identification performance and efficiency measurement with $t\bar{t}$ events in pp collisions at $\sqrt{s}$ = 13 TeV," *Eur. Phys. J. C* **79** (2019) 970, arXiv:1907.05120 [hep-ex].

[233] ATLAS Collaboration, "Measurements of b-jet tagging efficiency with the ATLAS detector using $t\bar{t}$ events at $\sqrt{s} = 13$ TeV," *JHEP* **08** (2018) 089, arXiv:1805.01845 [hep-ex].

[234] ATLAS Collaboration, "Performance of missing transverse momentum reconstruction with the ATLAS detector using proton–proton collisions at $\sqrt{s} = 13$ TeV," *Eur. Phys. J. C* **78** (2018) 903, arXiv:1802.08168 [hep-ex].

[235] ATLAS Collaboration, "$E_{\mathrm{T}}^{\mathrm{miss}}$ performance in the ATLAS detector using 2015-2016 LHC p-p collisions," Tech. Rep. ATLAS-CONF-2018-023, CERN, Geneva, Jun, 2018. http://cds.cern.ch/record/2625233.

[236] D. Adams *et al.*, "Recommendations of the Physics Objects and Analysis Harmonisation Study Groups 2014," Tech. Rep. ATL-PHYS-INT-2014-018, CERN, Geneva, Jul, 2014. https://cds.cern.ch/record/1743654.

[237] M. Cacciari, G. P. Salam, and G. Soyez, "The Catchment Area of Jets," *JHEP* **04** (2008) 005, arXiv:0802.1188 [hep-ph].

[238] UA1 Collaboration, "Experimental Observation of Isolated Large Transverse Energy Electrons with Associated Missing Energy at $\sqrt{s} = 540$ GeV," *Phys. Lett. B* **122** (1983) 103–116.

[239] Aachen-Annecy-Birmingham-CERN-Helsinki-London(QMC)-Paris(CdF)-Riverside-Rome-Rutherford-Saclay(CEN)-Vienna Collaboration, G. Arnison *et al.*, "Further evidence for charged intermediate vector bosons at the SPS collider," *Phys. Lett. B* **129** no. CERN-EP-83-111, (Jun, 1985) 273–282. 17 p. https://cds.cern.ch/record/163856.

[240] U. Baur, "Measuring the W boson mass at hadron colliders," in *Mini-Workshop on Electroweak Precision Data and the Higgs Mass*. 4, 2003. arXiv:hep-ph/0304266.

[241] J. Smith, W. L. van Neerven, and J. A. M. Vermaseren, "The Transverse Mass and Width of the W Boson," *Phys. Rev. Lett.* **50** (1983) 1738.

[242] D. R. Tovey, "On measuring the masses of pair-produced semi-invisibly decaying particles at hadron colliders," *JHEP* **04** (2008) 034, arXiv:0802.2879 [hep-ph].

[243] G. Polesello and D. R. Tovey, "Supersymmetric particle mass measurement with the boost-corrected contransverse mass," *JHEP* **03** (2010) 030, arXiv:0910.0174 [hep-ph].

[244] ATLAS Collaboration, "Performance of the missing transverse momentum triggers for the ATLAS detector during Run-2 data taking," *JHEP* **08** (2020) 080, arXiv:2005.09554 [hep-ex].

[245] ATLAS Collaboration, "Performance of algorithms that reconstruct missing transverse momentum in $\sqrt{s} = 8$ TeV proton-proton collisions in the ATLAS detector," *Eur. Phys. J. C* **77** no. 4, (2017) 241, arXiv:1609.09324 [hep-ex].

[246] ATLAS Collaboration, "ATLAS data quality operations and performance for 2015–2018 data-taking," *JINST* **15** (2020) P04003, arXiv:1911.04632 [physics.ins-det].

[247] ATLAS Collaboration, "Selection of jets produced in 13 TeV proton–proton collisions with the ATLAS detector." ATLAS-CONF-2015-029, 2015. https://cds.cern.ch/record/2037702.

[248] N. Hartmann, "ahoi." https://gitlab.com/nikoladze/ahoi, 2018.

[249] ATLAS Collaboration, "Object-based missing transverse momentum significance in the ATLAS detector," Tech. Rep. ATLAS-CONF-2018-038, CERN, Geneva, Jul, 2018. https://cds.cern.ch/record/2630948.

[250] A. Roodman, "Blind analysis in particle physics," *eConf* **C030908** (2003) TUIT001, arXiv:physics/0312102.

[251] W. Buttinger, "Using Event Weights to account for differences in Instantaneous Luminosity and Trigger Prescale in Monte Carlo and Data," tech. rep., CERN, Geneva, May, 2015. https://cds.cern.ch/record/2014726.

[252] ATLAS Collaboration, "Measurement of the Inelastic Proton–Proton Cross Section at $\sqrt{s} = 13$ TeV with the ATLAS Detector at the LHC," *Phys. Rev. Lett.* **117** (2016) 182002, arXiv:1606.02625 [hep-ex].

[253] ATLAS Collaboration, "A method for the construction of strongly reduced representations of ATLAS experimental uncertainties and the application thereof to the jet energy scale." ATL-PHYS-PUB-2015-014, 2015. https://cds.cern.ch/record/2037436.

[254] J. Bellm *et al.*, "Herwig 7.0/Herwig++ 3.0 release note," *Eur. Phys. J.* **C76** no. 4, (2016) 196, arXiv:1512.01178 [hep-ph].

[255] ATLAS Collaboration, "Simulation of top-quark production for the ATLAS experiment at $\sqrt{s} = 13$ TeV." ATL-PHYS-PUB-2016-004, 2016. https://cds.cern.ch/record/2120417.

[256] S. Frixione, E. Laenen, P. Motylinski, *et al.*, "Single-top hadroproduction in association with a W boson," *JHEP* **07** (2008) 029, arXiv:0805.3067 [hep-ph].

[257] ATLAS Collaboration, "SUSY July 2020 Summary Plot Update," Tech. Rep. ATL-PHYS-PUB-2020-020, CERN, Geneva, Jul, 2020. http://cds.cern.ch/record/2725258.

[258] CMS Collaboration, "Search for chargino-neutralino production in final states with a Higgs boson and a W boson," Tech. Rep. CMS-PAS-SUS-20-003, CERN, Geneva, 2021. https://cds.cern.ch/record/2758360.

[259] ATLAS Collaboration, "Search for electroweak production of charginos and sleptons decaying into final states with two leptons and missing transverse momentum in $\sqrt{s} = 13$ TeV pp collisions using the ATLAS detector," *Eur. Phys. J. C* **80** (2020) 123, arXiv:1908.08215 [hep-ex].

[260] G. Apollinari, I. Béjar Alonso, O. Brüning, *et al.*, *High-Luminosity Large Hadron Collider (HL-LHC): Preliminary Design Report*. CERN Yellow Reports: Monographs. CERN, Geneva, 2015. https://cds.cern.ch/record/2116337.

[261] X. Chen, S. Dallmeier-Tiessen, R. Dasler, *et al.*, "Open is not enough," *Nature Physics* **15** no. 2, (Feb, 2019) 113–119. https://doi.org/10.1038/s41567-018-0342-2.

[262] LHC Reinterpretation Forum Collaboration, W. Abdallah *et al.*, "Reinterpretation of LHC Results for New Physics: Status and Recommendations after Run 2," *SciPost Phys.* **9** no. 2, (2020) 022, arXiv:2003.07868 [hep-ph].

[263] ATLAS Collaboration, "RECAST framework reinterpretation of an ATLAS Dark Matter Search constraining a model of a dark Higgs boson decaying to two b-quarks." ATL-PHYS-PUB-2019-032, 2019. https://cds.cern.ch/record/2686290.

[264] K. Cranmer and I. Yavin, "RECAST: Extending the Impact of Existing Analyses," *JHEP* **04** (2011) 038, arXiv:1010.2506 [hep-ex].

[265] D. Dercks, N. Desai, J. S. Kim, *et al.*, "CheckMATE 2: From the model to the limit," *Comput. Phys. Commun.* **221** (2017) 383–418, arXiv:1611.09856 [hep-ph].

[266] M. Drees, H. Dreiner, D. Schmeier, *et al.*, "CheckMATE: Confronting your Favourite New Physics Model with LHC Data," *Comput. Phys. Commun.* **187** (2015) 227–265, arXiv:1312.2591 [hep-ph].

[267] E. Conte, B. Fuks, and G. Serret, "MadAnalysis 5, A User-Friendly Framework for Collider Phenomenology," *Comput. Phys. Commun.* **184** (2013) 222–256, arXiv:1206.1599 [hep-ph].

[268] E. Maguire, L. Heinrich, and G. Watt, "HEPData: a repository for high energy physics data," *J. Phys. Conf. Ser.* **898** no. 10, (2017) 102006, arXiv:1704.05473 [hep-ex].

[269] ATLAS Collaboration, "Simpleanalysis." https://gitlab.cern.ch/atlas-sa/simple-analysis, 2021.

[270] S. Ovyn, X. Rouby, and V. Lemaitre, "DELPHES, a framework for fast simulation of a generic collider experiment," arXiv:0903.2225 [hep-ph].

[271] A. Buckley, J. Butterworth, D. Grellscheid, *et al.*, "Rivet user manual," *Comput. Phys. Commun.* **184** (2013) 2803–2819, arXiv:1003.0694 [hep-ph].

[272] A. Buckley, D. Kar, and K. Nordström, "Fast simulation of detector effects in Rivet," *SciPost Phys.* **8** (2020) 025, arXiv:1910.01637 [hep-ph].

[273] S. Kraml, S. Kulkarni, U. Laa, *et al.*, "SModelS: a tool for interpreting simplified-model results from the LHC and its application to supersymmetry," *Eur. Phys. J. C* **74** (2014) 2868, arXiv:1312.4175 [hep-ph].

[274] F. Ambrogi, S. Kraml, S. Kulkarni, *et al.*, "SModelS v1.1 user manual: Improving simplified model constraints with efficiency maps," *Comput. Phys. Commun.* **227** (2018) 72–98, arXiv:1701.06586 [hep-ph].

[275] ATLAS Collaboration, "Search for direct production of electroweakinos in final states with one lepton, missing transverse momentum and a higgs boson decaying into two b-jets in pp collisions at $\sqrt{s}$ = 13 tev with the atlas detector," 2021. https://www.hepdata.net/record/ins1755298?version=4.

[276] ATLAS Collaboration, "1lbb-likelihoods-hepdata.tar.gz," 2020. https://www.hepdata.net/record/resource/1408476?view=true.

[277] G. Alguero, S. Kraml, and W. Waltenberger, "A SModelS interface for pyhf likelihoods," arXiv:2009.01809 [hep-ph].

[278] M. D. Goodsell, "Implementation of the ATLAS-SUSY-2019-08 analysis in the MadAnalysis 5 framework (electroweakinos with a Higgs decay into a $b\bar{b}$ pair, one lepton and missing transverse energy; 139 fb^{-1})," *Mod. Phys. Lett. A* **36** no. 01, (2021) 2141006.

[279] J. Y. Araz *et al.*, "Proceedings of the second MadAnalysis 5 workshop on LHC recasting in Korea," *Mod. Phys. Lett. A* **36** no. 01, (2021) 2102001, arXiv:2101.02245 [hep-ph].

[280] M. Feickert, L. Heinrich, G. Stark, and B. Galewsky, "Distributed statistical inference with pyhf enabled through funcX," in *25th International Conference on Computing in High-Energy and Nuclear Physics*. 3, 2021. arXiv:2103.02182 [cs.DC].

[281] R. Chard, Y. Babuji, Z. Li, *et al.*, "funcx: A federated function serving fabric for science," ACM, Jun, 2020. http://dx.doi.org/10.1145/3369583.3392683.

[282] D. Merkel, "Docker: Lightweight linux containers for consistent development and deployment," *Linux J.* **2014** no. 239, (Mar., 2014) .

[283] S. Binet and B. Couturier, "docker & HEP: Containerization of applications for development, distribution and preservation," *J. Phys.: Conf. Ser.* **664** no. 2, (2015) 022007. 8 p. https://cds.cern.ch/record/2134524.

[284] K. Cranmer and L. Heinrich, "Yadage and Packtivity - analysis preservation using parametrized workflows," *J. Phys. Conf. Ser.* **898** no. 10, (2017) 102019, arXiv:1706.01878 [physics.data-an].

[285] E. R. Gansner and S. C. North, "An open graph visualization system and its applications to software engineering," *SOFTWARE - PRACTICE AND EXPERIENCE* **30** no. 11, (2000) 1203–1233.

[286] E. R. Gansner, Y. Koren, and S. North, "Graph drawing by stress majorization," in *Graph Drawing*, J. Pach, ed., pp. 239–250. Springer Berlin Heidelberg, Berlin, Heidelberg, 2005.

[287] ATLAS Collaboration, "Electron and photon energy calibration with the ATLAS detector using 2015–2016 LHC proton–proton collision data," *JINST* **14** (2019) P03017, arXiv:1812.03848 [hep-ex].

[288] Schanet, Eric, "simplify," Version 0.1.5. https://github.com/eschanet/simplify.

[289] Schanet, Eric, "SUSY-2019-08 simplified likelihood," Version 0.0.1. https://github.com/eschanet/simplify/blob/master/examples/ANA-SUSY-2019-08/simplify_BkgOnly.json.

[290] P. C. Bryan and M. Nottingham, "Javascript object notation (json) patch," Version RFC 6902, Apr, 2013. https://www.rfc-editor.org/rfc/rfc6902.txt.

[291] ATLAS Collaboration, "Search for direct stau production in events with two hadronic τ-leptons in $\sqrt{s} = 13$ TeV pp collisions with the ATLAS detector," *Phys. Rev. D* **101** (2020) 032009, arXiv:1911.06660 [hep-ex].

[292] ATLAS Collaboration, "Search for bottom-squark pair production with the ATLAS detector in final states containing Higgs bosons, b-jets and missing transverse momentum," *JHEP* **12** (2019) 060, arXiv:1908.03122 [hep-ex].

[293] W. Porod, "SPheno, a program for calculating supersymmetric spectra, SUSY particle decays and SUSY particle production at e+ e- colliders," *Comput. Phys. Commun.* **153** (2003) 275–315, arXiv:hep-ph/0301101.

[294] W. Porod and F. Staub, "SPheno 3.1: Extensions including flavour, CP-phases and models beyond the MSSM," *Comput. Phys. Commun.* **183** (2012) 2458–2469, arXiv:1104.1573 [hep-ph].

[295] S. Heinemeyer, W. Hollik, and G. Weiglein, "FeynHiggs: A Program for the calculation of the masses of the neutral CP even Higgs bosons in the MSSM," *Comput. Phys. Commun.* **124** (2000) 76–89, arXiv:hep-ph/9812320.

[296] H. Bahl, T. Hahn, S. Heinemeyer, *et al.*, "Precision calculations in the MSSM Higgs-boson sector with FeynHiggs 2.14," *Comput. Phys. Commun.* **249** (2020) 107099, arXiv:1811.09073 [hep-ph].

[297] T. Hahn, S. Heinemeyer, W. Hollik, *et al.*, "High-Precision Predictions for the Light CP -Even Higgs Boson Mass of the Minimal Supersymmetric Standard Model," *Phys. Rev. Lett.* **112** no. 14, (2014) 141801, arXiv:1312.4937 [hep-ph].

[298] B. C. Allanach, "SOFTSUSY: a program for calculating supersymmetric spectra," *Comput. Phys. Commun.* **143** (2002) 305–331, arXiv:hep-ph/0104145 [hep-ph].

[299] G. Belanger, F. Boudjema, A. Pukhov, and A. Semenov, "MicrOMEGAs 2.0: A Program to calculate the relic density of dark matter in a generic model," *Comput. Phys. Commun.* **176** (2007) 367–382, arXiv:hep-ph/0607059.

[300] G. Belanger, F. Boudjema, A. Pukhov, and A. Semenov, "micrOMEGAs: A Tool for dark matter studies," *Nuovo Cim. C* **033N2** (2010) 111–116, arXiv:1005.4133 [hep-ph].

[301] W. Beenakker, R. Hopker, and M. Spira, "PROSPINO: A Program for the Production of Supersymmetric Particles in Next-to-leading Order QCD," Tech. Rep. hep-ph/9611232, Nov, 1996. https://cds.cern.ch/record/314229. 12 pages, latex, no figures, Complete postscript file and FORTRAN source codes available from http://wwwcn.cern.ch/ mspira/prospino/.

[302] W. Beenakker, M. Klasen, M. Kramer, *et al.*, "The Production of charginos / neutralinos and sleptons at hadron colliders," *Phys. Rev. Lett.* **83** (1999) 3780–3783, arXiv:hep-ph/9906298. [Erratum: Phys.Rev.Lett. 100, 029901 (2008)].

[303] ATLAS Collaboration, "Search for long-lived charginos based on a disappearing-track signature using 136 fb^{-1} of pp collisions at $\sqrt{s}$ = 13 TeV with the ATLAS detector," Tech. Rep. ATLAS-CONF-2021-015, CERN, Geneva, Mar, 2021. https://cds.cern.ch/record/2759676.

[304] A. Arbey, M. Battaglia, and F. Mahmoudi, "Higgs Production in Neutralino Decays in the MSSM - The LHC and a Future e^+e^- Collider," *Eur. Phys. J. C* **75** no. 3, (2015) 108, arXiv:1212.6865 [hep-ph].

[305] M. E. Cabrera, J. A. Casas, A. Delgado, *et al.*, "Naturalness of MSSM dark matter," *JHEP* **08** (2016) 058, arXiv:1604.02102 [hep-ph].

[306] N. Arkani-Hamed, G. L. Kane, J. Thaler, and L.-T. Wang, "Supersymmetry and the LHC inverse problem," *JHEP* **08** (2006) 070, arXiv:hep-ph/0512190.

[307] S. Amari, *Differential-Geometrical Methods in Statistics.* Springer New York, New York, NY, 1985.

[308] J. Brehmer, K. Cranmer, F. Kling, and T. Plehn, "Better Higgs boson measurements through information geometry," *Phys. Rev. D* **95** no. 7, (2017) 073002, arXiv:1612.05261 [hep-ph].